Fighting tumor: general and prostate cancer models comparison

Stefano Costa, Elisa Muratore and Seyed Mohsen Moosavi

January 7, 2023

Introduction

Immunotherapy is defined as a therapeutic approach that targets or manipulates the immune system. Ultimately is under preliminary research for its potential to treat various forms of cancer: the goal of immunotherapy is to strengthen the body's own natural ability to combat cancer by enhancing the effectiveness of the immune system.

The importance of the immune system in fighting cancer has been verified in the laboratory as well as with clinical experiments (see *Mixed immunotherapy and chemotherapy of tumors: modeling, applications and biological interpretations* for a list of references), and has also been found in mathematical models: through the mathematical modeling of tumor growth, the presence of an immune component has been shown to be essential for producing clinically observed phenomena.

A cyclic behavior of tumor size has often been found in previous mathematical models and is directly attributable to the interaction of the tumor with the immune system.

The clear importance of the immune system in controlling cancer growth, both clinically and mathematically, indicates that models incorporating tumor growth and treatment would do well to include an immune system component.

Once this component is in place, it is then possible to model how various immunotherapies may affect the system, either singly or in combination with one another (for example in combination with vaccine therapy).

In this relation the first model, which regards a general cancer growth and the effect of immunotherapy, vaccine and chemotherapy treatments, was analysed by Stefano Costa. The second one, which specifically deals with prostate cancer and immunotherapy treatments, was examined by Elisa Muratore; finally, the comparison was made by Seyed Mohsen Moosavi. Clearly, although each section was written by an individual, the other components revised what was written by contributing and enriching the text with changes and additions. The models analysed within this report come from the following papers:

- de Pillis, Lisette G., Weiqing Gu, and Ami E. Radunskaya. "**Mixed immunotherapy and chemotherapy of tumors: modeling, applications and biological interpretations.**" Journal of theoretical biology 238.4 (2006): 841-862.
- Coletti, Roberta, Andrea Pugliese, and Luca Marchetti. "**Modeling the effect of immunotherapies on human castration-resistant prostate cancer.**" Journal of Theoretical Biology 509 (2021): 110500.

Other sources were consulted for some concepts. Especially to understand the difference between cell populations and some concepts of interaction between cells, so as to understand the reasons for adding some terms in the model. In order to speed up the writing process and because it is not the aim of the report, a complete bibliography of all the sources consulted was avoided, also because a quick consultation on the web was often enough to obviate our biological doubts.

1 De Pillis' model

The model proposed in the paper is useful for simulating tumor dormancy and sneaking through, situation in which the tumor appears to have disappeared only to reappear at lethal size through study of equilibria.

Assumption

The model is based on the previous one developed by de Pillis and exploits conclusions drawn from other published papers. Here we will not go into biological details to avoid going into too much detail: important assumptions for understanding the structure of the model will just be mentioned.
Biological assumptions made in the model are: tumor grows logistically in absence of immune response (based on fitted data, see paper for reference); NK and $CD8^+$T cells can kill tumor cells; NK cells are normally present in the body; $CD8^+$T cells are only present in large number when tumor cells are present; NK and $CD8^+$T cells become inactive after some number of encounter with tumor cells; source of NK cells is represented as a fraction of the circulating lymphocite population (a biological simplification); chemotherapy can kill tumor cells and NK and $CD8^+$T cells.

Model equation

The model describes the kinetics of four populations (tumor cells and three types of immune cells), as well as two drug concentrations in the bloodstream. The populations at time t are denoted by:

- $T(t)$ tumor cell population
- $N(t)$ total NK cell population
- $L(t)$ total $CD8^+$T cell population
- $C(t)$ number of circulating lymphocytes
- $M(t)$ chemotherapy drug concentration in the bloodstream
- $I(t)$ immunotherapy drug concentration in the bloodstream

The equations governing the population kinetics takes into account:

- A net growth term for each population: $(G_T, G_N, G_L, G_C, G_M, G_I)$
- The fractional cell kill: $(F_N, F_L, F_{MT}, F_{MN}, F_{ML}, F_{LI}, F_{CM})$
  The *fractional kill* represent the fraction of cell population that dies because of interaction with other populations of cell.
- Per cell recruitment: (R_N, R_L)
  The *cell recruitment* represent the interactions between $CD8^+$T and NK cells and tumor cells: dynamics of activation of one cell population for the other come into play.
- Cell inactivation: (I_N, I_L, I_{CL})
  The *cell inactivation* term plays the role of reducing the cell population when it no longer has an effect on cancer cells. When an NK or CD8+T cell is no longer able to fight the tumor they may incur cytolysis (cell bursts due to an osmotic imbalance), so the body inactivates them.
- External intervention with medication: (H_L, H_M, H_I)

Remark: the *fractional cell kill* rates are not only due to tumor cells, they are also caused by interaction between other non-malignant cell populations for example for competing for space, competing for nutrients, body regulation...
Remark: the population levels $N + L$ actually represent immune cell effectiveness in the sense that an increase may actually be evidenced biologically as a greater number of total cells or as each individual immune cell becoming more efficient at killing the tumor cells.

Overall, the model is as follows:

$$
\begin{aligned}
\frac{dT}{dt} &= aT(1-bT) - cNT - DT - K_T(1-e^{-M})T \\
\frac{dN}{dt} &= eC - fN + g\frac{T^2}{h+T^2}N - pNT - K_N(1-e^{-M})N \\
\frac{dL}{dt} &= -mL + j\frac{D^2T^2}{k+D^2T^2}L - qLT + (r_1N + r_2C)T - uNL^2 - K_L(1-e^{-M})L + \frac{p_I LI}{g_I + I} + v_L(t) \\
\frac{dC}{dt} &= \alpha - \beta C - K_C(1-e^{-M})C \\
\frac{dM}{dt} &= -\gamma M + v_M(t) \qquad \frac{dI}{dt} = -\mu_I I + v_I(t) \qquad D = d\frac{(L/T)^l}{s+(L/T)^l}
\end{aligned}
$$

Each equation of the model is now explained in detail:

$$
\frac{dT}{dt} = \overbrace{aT(1-bT)}^{G_T} - \overbrace{cNT}^{F_N(T,N)} - \overbrace{DT}^{F_L(T,L)} - \overbrace{K_T(1-e^{-M})T}^{F_{MT}}
$$

The logistic growth G_T of tumor is based on data gathered from immunodeficient mice (see the paper for reference). The F_N and F_L terms are taken from a previous model of the same authors and have a form that can describe well experimental data tested by the authors in previous publications (see the paper for references). The F_L term depends on the function $D(T,L) = d\frac{(L/T)^l}{s+(L/T)^l}$, which represent the tumor cells lysed (destroyed membrane) by CD8$^+$T cells. The action of chemotherapy affects all cell populations but its efficacy is bounded. Therefore a saturation term is used and represented by the $1-e^{-M}$ term; this term is then multiplied by a different coefficient for each cell population.

Remark: although the term D is reminiscent of the Holling type 3 response, because it depends not only on "prey" (in this case T) but also on "predators" (in this case L) it cannot be defined as such. Moreover, compared to the function we have seen the Holling response play, a different role is played here.
Remark: the $F_{M\phi}$ term ($\phi = T, N, L, C$) at low concentration of drug is nearly linear, while at higher concentration the kill rate plateaus.

$$
\frac{dN}{dt} = \overbrace{eC - fN}^{G_N} + \overbrace{\frac{gT^2}{h+T^2}N}^{R_N(T,N)} - \overbrace{pNT}^{I_N} - \overbrace{K_N(1-e^{-M})N}^{F_{MN}}
$$

The growth term is tied to C (overall lymphocytes circulating) because this allows the simulation of chemotherapy, in which there is a suppression of stem cells which lowers C and affects the production rate of N. Hence the growth rate is made by the natural death rate of cells (negative exponential) coupled with a term depending linearly on C. The recruitment term $R_N(T,N)$ is taken from other models (see the paper for references) and it is basically a Michaelis-Mentel equation in 2-binding-site enzymatic cooperation (where what we've called K_m is now $\sqrt{h}$) with T as the substrate[1]. The inactivation term I_N is taken from other models (see paper for reference), the parameter represent mean inactivation rates.

Remark: G_N was taken constant in a previous model of the same author, but that did not give the possibility to simulate the action of drugs. Therefore, this assumption was modified to increase the possibilities of the model

$$
\frac{dL}{dt} = \overbrace{-mL}^{G_L} + \overbrace{\frac{jD^2T^2}{k+D^2T^2}L}^{R_L^1(T,L)} - \overbrace{qLT}^{I_L} + \overbrace{r_1NT}^{R_L^2(N,T)} + \overbrace{r_2CT}^{R_L^3(C,T)} - \overbrace{uNL^2}^{I_{CL}} - \overbrace{K_L(1-e^{-M})L}^{F_{ML}} + \overbrace{\frac{p_I I}{g_I + I}L}^{F_{LI}} + \overbrace{v_L(t)}^{H_L}
$$

It is assumed that no CD8$^+$T cells are present in absence of tumor cells, so a negative exponential growth is used, which represent the natural death rate of cells.
Taking the F_{LI} term from a model developed by other authors (see the paper for references), CD8$^+$T activation by immunotherapy is included in the equation, which occurs according to the dynamics of the Michaelis-Mentel law.
To give a detailed explanation, the recruitment term is divided into three parts.
CD8$^+$T cells require different triggers to be activated, including the number of tumor cells lysed by themselves. So the recruitment term R_L^1 is similar to the R_N term in which T is replaced with D, so the tumor cells lysed by CD8$^+$T cells.
CD8$^+$T cells can also be recruited by debris from tumor cells lysed by NK cells. To model this aspect, the R_L^2 term

[1]In the paper, the form of this term is called a *modified Michaelis-Menten* without mentioning whether there is a form of cooperative enzymatic relationship between NK and tumor cells. Delving into this biological aspect of interaction between the two cell populations takes time and we believe it is beyond the scope of this research; therefore, we decided not to investigate the biological origin of this term.

for recruiting is proportional to the number of cells killed.
Also CD8$^+$T cells are produced based on presence of tumor cells. So the R_L^3 term is proportional to the average number of encounter between circulating lynphocytes and tumor cells.
The inactivation term I_L is taken from other models (see paper for reference). The I_{CL} term describes regulation of CD8$^+$T cells when they are too many; NK cells aid in the deactivation.
The drug intervention term H_L represents an immunotherapy in which the immune cell levels are boosted.

$$\frac{dC}{dt} = \overbrace{\alpha - \beta C}^{G_C} - \overbrace{K_C(1 - e^{-M})C}^{F_{MC}}$$

For C a simple hypothesis is made: circulating lymphocytes are generated at a constant rate (α term) and have a natural lifespan ($-\beta C$ term).

$$\frac{dM}{dt} = \overbrace{-\gamma M}^{G_M} + \overbrace{v_M(t)}^{H_M}$$

It is assumed that after injection, the chemotherapy drug will be eliminated from the body at a rate proportional to its concentration, hence an exponential decay is assumed.
The drug intervention term H_M reflect the amount of chemotherapy drug given over time.

$$\frac{dI}{dt} = \overbrace{-\mu_I I}^{G_I} + \overbrace{v_I(t)}^{H_I}$$

The same assumption is made for the growth factor of immunotherapy as is made for chemotherapy.
The drug intervention term H_I reflect the amount of immunotherapy drug given over time.

Parameters value

The topic of parameter values is partially beyond the scope of this report. It is important to emphasize how the various constant parameters mentioned in the equations differ for different cancers and for each individual (human and animal). In the source (and also by us) experimental values estimated from other papers on humans and mice are used. For details of the values and biological/cellular considerations, see the tables accompanying the paper.

Non-dimensionalization

To allow for analysis we suppose $M = 0$ and $I = 0$ (no immunotherapy nor chemotherapy) and we non-dimensionalize the previous system as follows:

$$C^* = \frac{a}{\alpha}C \qquad T^* = bT \qquad N^* = \frac{a^2}{\alpha e}N \qquad L^* = bL \qquad D^* = \frac{1}{a}D \qquad t^* = at$$

Remark: time is reparametrized according to the growth rate of tumor cells so that, together with reparameterization of T^*, we obtain a "normalized" logistic growth ($r = 1$, $K = 1$) for tumor cells, which is the cell population that we are most interested in.

The parameters are:

$$c^* = \frac{c\alpha e}{a^3} \qquad d^* = \frac{d}{a} \qquad f^* = \frac{f}{a} \qquad g^* = \frac{g}{a} \qquad h^* = hb^2 \qquad j^* = \frac{j}{a} \qquad k^* = \frac{kb^2}{a}$$

$$m^* = \frac{m}{a} \qquad p^* = \frac{p}{ab} \qquad q^* = \frac{q}{ba} \qquad r_1^* = \frac{r_1\alpha e}{a^3} \qquad r_2^* = \frac{r_2\alpha}{a^2} \qquad s^* = s \qquad u^* = \frac{u\alpha e}{a^3 b} \qquad \beta^* = \frac{\beta}{a}$$

Removing the stars for notational clarity we obtain:

$$\frac{dT}{dt} = T(1 - T) - cNT - DT \qquad \frac{dN}{dt} = C - fN + g\frac{T^2}{h + T^2}N - pNT$$

$$\frac{dC}{dt} = 1 - \beta C \qquad D = d\frac{(L/T)^l}{s + (L/T)^l}$$

$$\frac{dL}{dt} = -mL + j\frac{D^2T^2}{k + D^2T^2}L - qLT + (r_1N + r_2C)T - uNL^2$$

Equilibria

First we notice that the equation for dC/dt decouples from dT/dt, dN/dt, dL/dt. So we find that at equilibrium $C_E = 1/\beta$. We set now the other three differential equation to zero to find the equilibria. First we notice that dT/dt have two equilibria: $T_{E,1} = 0$ and $T_{E,2} \neq 0$. The tumor-free equilibrium is $E_0 = (T_{E,1}, N_E, L_E, C_E) = (0, 1/\beta f, 0, 1/\beta)$. The $T_{E,2}$ case require numerical analysis of the system. From $dN/dt = 0$ we obtain:

$$N_E = \frac{C_E(h + T^2)}{fh + (f - g)T^2 + phT + pT^3}$$

Since we cannot obtain an analytical solution, we want to intersect the other equations. In order to do so, we reduce them as function of T and L. From $dT/dt = 0$ we obtain D_E that we apply then to the equation for D:

$$D_E = 1 - T - N_E \qquad \Rightarrow \qquad L_{E,l} = \left(\frac{D_E s T^l}{d - D_E}\right)^{1/l}$$

Finally from $dL/dt = 0$ we obtain:

$$L^2(uN_E) + L\left(m - \frac{jD_E^2T^2}{k + D_E^2T^2 + qT}\right) - (r_1N_E + r_2C_E)T = 0$$

In order to find equilibrium points we intersect the last equation with the expression of $L_{E,l}$.

From what we obtain there can be multiple non-zero tumor equilibrium points. For the estimated set of mouse parameters, although there are two solutions, there is only one positive (biologically relevant) solution (see the paper for details, Fig. 1 in particular): $T_E \approx 3.48 \times 10^7$. This means that (for a mouse) the tumor will growth at most on the order of 10^7 cells.

Stability

Stability of the equilibria are determined by linearizing the system and studying the jacobian.

The stability of equilibria is important from a physiological viewpoint: if the system is at equilibrium but the equilibrium point is unstable, a small perturbation from equilibrium will cause the system to move away from that point and evolve toward the stable equilibrium, as in figure 1.

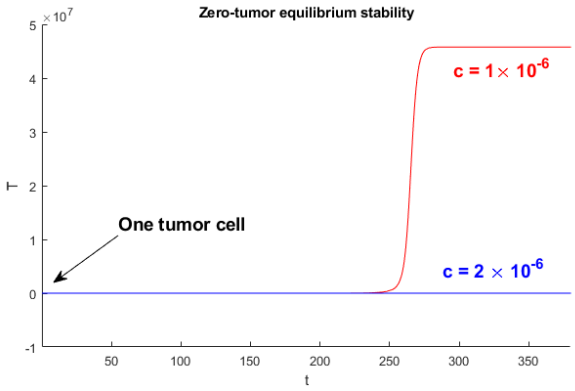

Figure 1: In this simulations two values of c are taken: in one case the zero-tumor equilibrium is stable, in the other case is unstable. In the unstable case, it can be seen in the graph that starting from a single tumor cell after some time the tumor grows to up to carrying capacity. In the stable case the tumor will die. The graph was made with matcont from different initial values than in the paper: $T_0 = 1$, $N_0 = 10^6$, $C = 10^7$, $L_0 = 0$, in order to obtain it we simplify the system nullifying immune recruitment parameters: $g = j = r_1 = r_2 = 0$.

In figure 1, in the red case the tumor-free equilibrium is unstable while the high-tumor equilibrium is stable. This means that if the treatment is stopped the system will inevitably return to the high-tumor state, meaning that the tumor will escape the immunoresponse. In this case with only two equilibria, this implies that to be effective, a cure must kill all the tumor cells and change the other value of the system. This phenomena can also be seen in figure 2.

Therefore, the role of immunotherapy might be interpreted in this context as a treatment which changes system parameters by, for example, raising the *kill potential* of the NK cells.

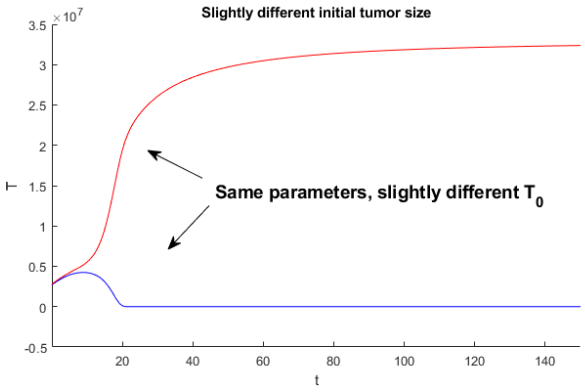

Figure 2: In this simulations $c = 2 \times 10^{-6}$, so the zero-tumor equilibrium is unstable. In blue is the case when the treatment can kill all the tumor cell. If that is not the case, as in red, since the tumor-high equilibrium is stable, the tumor still grows up to carrying capacity. In this case the system is highly susceptible to small changes: the T_0 here changes only by little. Also in this case the values for initial point are different from the paper: $T_0^{\text{red}} = 2.8 \times 10^6$, $T_0^{\text{blue}} = 2.7 \times 10^6$, $N_0 = 5 \times 10^4$, $L_0 = 5 \times 10^3$, $C_0 = 5 \times 10^4$.

The jacobian at the tumor-free equilibrium is:

$$J(E_0) = \begin{pmatrix} 1 - \frac{c}{\beta f} & 0 & 0 \\ -\frac{p}{\beta f} & -f & 0 \\ \frac{r_1}{\beta f} + \frac{r_2}{\beta} & 0 & -m \end{pmatrix}$$

Hence the eigenvalues are: $\lambda_1 = 1 - \frac{c}{\beta f}$, $\lambda_2 = -f < 0$ and $\lambda_3 = -m < 0$. So the tumor-free equilibrium is stable if and only if $\lambda_1 < 0 \Leftrightarrow c > \beta f$, hence it depends on the value of c, that represents the NK cells kill rate. Hence a bifurcation diagram depending on c can be made, as shown in figure 3.
Remark: since we are not working in two dimensions, we cannot analyze the properties of determinant and trace. We are forced to use the theorem on linearization of systems, which assures us that sufficient condition to have local asymptotic stability is to have eigenvalues strictly less than zero.

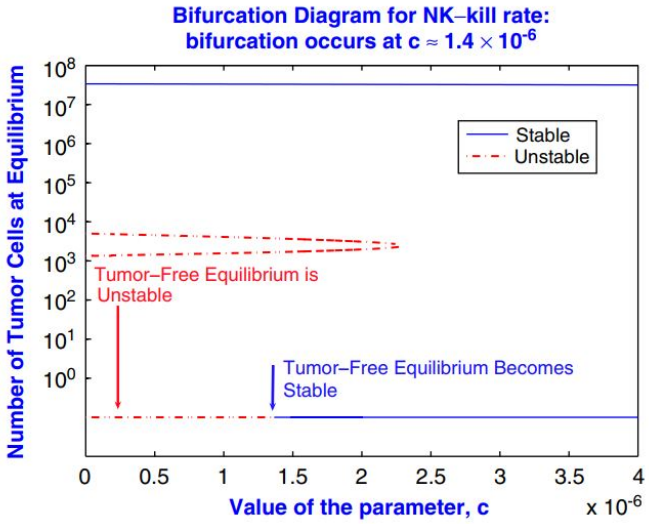

Figure 3: Bifurcation diagram showing the effect of varying c (NK kill rate). For all parameters value specification see the paper, Fig. 2

The bifurcation diagram shows the disappearance of two unstable non-zero tumor equilibria and the stabilization of the tumor-free equilibrium as the parameter c is increased. Recalling the c represent the kill rate, the effectiveness of NK cells killing tumor cells, we expected this behavior.

A bifurcation diagram can also be done with the j parameter, which appears in the recruitment term in dL/dt, so represents the strength of immune response.

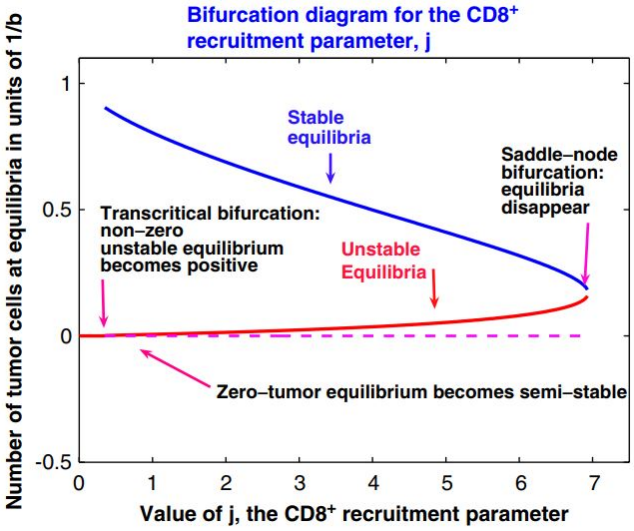

Figure 4: Bifurcation diagram showing the effect of varying j (strength of immune response). For all parameters value specification see the paper, Fig. 2

Two bifurcations are evident in the diagram: the first is a transcritical bifurcation, where the negative equilibrium becomes positive, and the zero-tumor equilibrium changes its stability. [2]

Before the bifurcation, the zero-tumor equilibrium is strictly unstable: (mathematically) even one tumor cell will result in the system moving toward the high-tumor equilibrium. After the bifurcation the zero-tumor becomes semi-stable

Remark: we have not seen in class the *semi-stable* equilibrium. An equilibrium solution $y(t)$ is **semi-stable** if initial conditions on one side of $y(t)$ lead to solutions that approach $y(t)$ as $t \to \infty$, while solution with initial conditions on the other side do not approach $y(t)$ itself, as shown in figure 5.

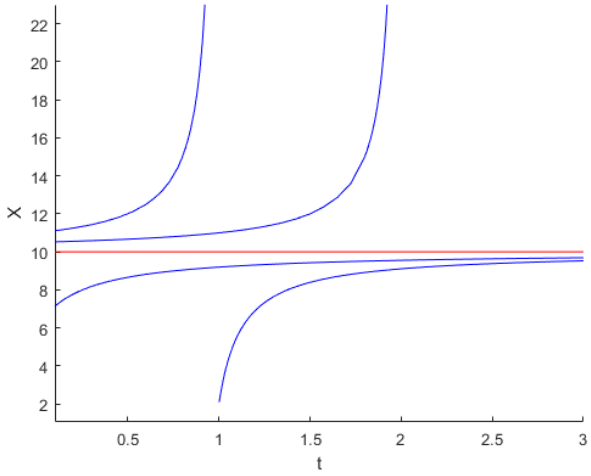

Figure 5: Example of semi-stable equilibrium made in matcont. In the simple system $x' = (x-10)^2$ the $x = 10$ is a semistable equilibrium since starting below it lead to convergence to equilbrium, while starting above it lead to divergence.

In the tumor model we are not in low dimensions, so we have no *above* nor *below*, but there is a *basin of attraction* for the zero-tumor equilibria, meaning that after the bifurcation, the immune system is able to control small initial tumor populations.

Figure 6 highlights the fact that even if the tumor is very small, extremely low $CD8^+T$ levels will allow the tumor to escape immune surveillance. The location of the basin boundary is therefore crucial in determining the outcome of

[2] It can be hard to spot, but for $j \approx 0$ there is only the red curve, indicating the unstability of the zero-tumor. At roughly $j \approx 0.3$ it appears the pink dashed line, which represent the change in stability of the zero-tumor equilibrium, that is now semi stable.

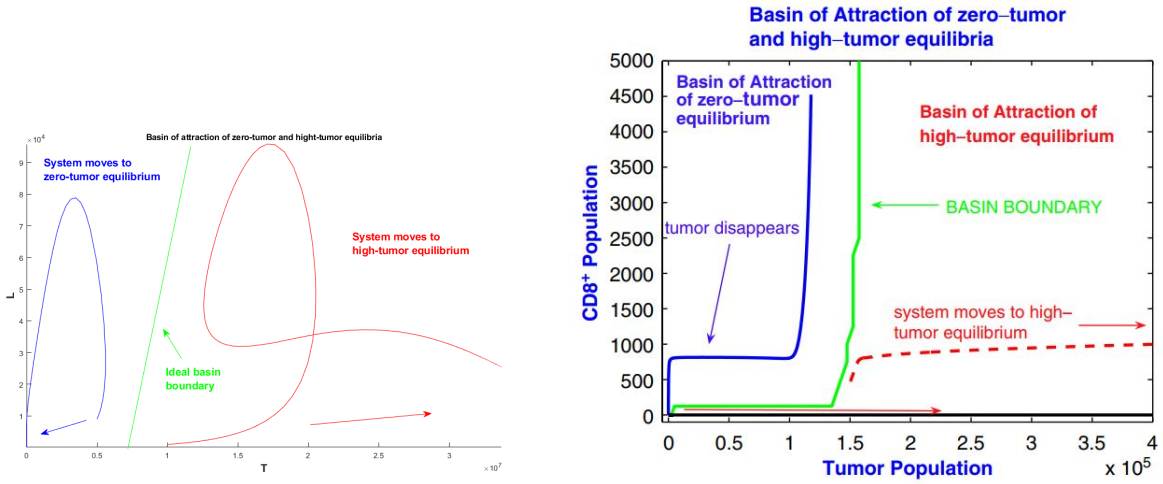

Figure 6: Basin of attraction of the zero-tumor and high-tumor equilibria. The left one is the one made in matcont where: $T_0^{\text{red}} = 10^7$, $N_0^{\text{red}} = 0$, $L_0^{\text{red}} = 10^3$, $C_0^{\text{red}} = 0$; $T_0^{\text{blue}} = 5 \times 10^6$, $N_0^{\text{blue}} = 10$, $L_0^{\text{blue}} = 9 \times 10^3$, $C_0^{\text{blue}} = 10$; since the graph shown in the paper is perhaps more "beautiful" and more intuitive to understand, that is also shown on the right; in which $j = 4.5$, $N = N_E$ and $C = C_E$

the disease.
In the case of a patient who has undergone chemotherapy which reduces both tumor and CD8$^+$T cell levels, if these levels place the system below the basin boundary then even an undetectable tumor will regrow. However, if the patient is given immunotherapy subsequent to chemotherapy, thereby boosting CD8$^+$T levels above the basin boundary, the system will evolve toward the stable zero-tumor equilibrium, and the tumor will not regrow. This hypothetical scenario emphasizes the potential importance of combination therapy.

Numerical experiment: human data with immunotherapy, chemotherapy and combination treatments

In this section we replicate what is done in the paper: we test the complete model (thus with the immunotherapy and chemotherapy components) using parameters measured in human patients to analyze different treatment situations.

As previously, it was very difficult to replicate the same results obtained in terms of graphs since using the same values given by the authors to accompany the images did not provide the same results. Substantial changes had to be made in the choice of parameters that tended to weaken the results obtained: smaller starting tumor size, better starting immune conditions or more potent drugs (in terms of the amount of administered...)

We understand that we cannot expect the same exact results as the researchers as many parameters influence the results (numerical precision, programming language and program used...) but we criticize the lack of clarity towards the methods used to obtain the numerical results, which would make the conclusions obtained reproducible, a very important factor in the scientific world.

Immune system response

This simulation represents a situation in which the immune system has not become activated against the tumor cell population until the population has reached 10^6 cells (still considered as below the threshold of clinical detectability). As we see in the simulations, the immune system plays a key role in the absence of therapies: it is precisely the difference in the starting values of NK, $CD8^+T$, and lymphocytic cell populations that determines patient survival. As seen in figure 33, the healthy innate immune response is sufficiently strong to control the tumor.

However, when the immune system is weakened, a tumor of the same size grows to a dangerous level in the absence of treatment interventions. This is the case of figure 8.

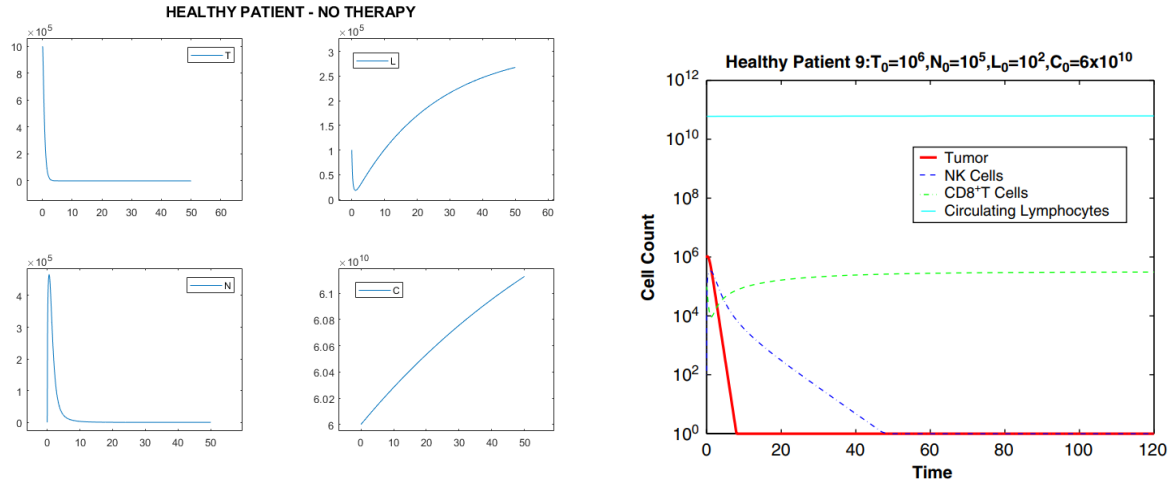

Figure 7: Left: generated in matlab with ode45. Right: figure 7 (left) in the paper. For both: $T_0 = 10^6$; $N_0 = 10^5$; $L_0 = 100$; $C_0 = 6 \times 10^{10}$. The parameters are the one reported in table 2 in the paper, patient 9.

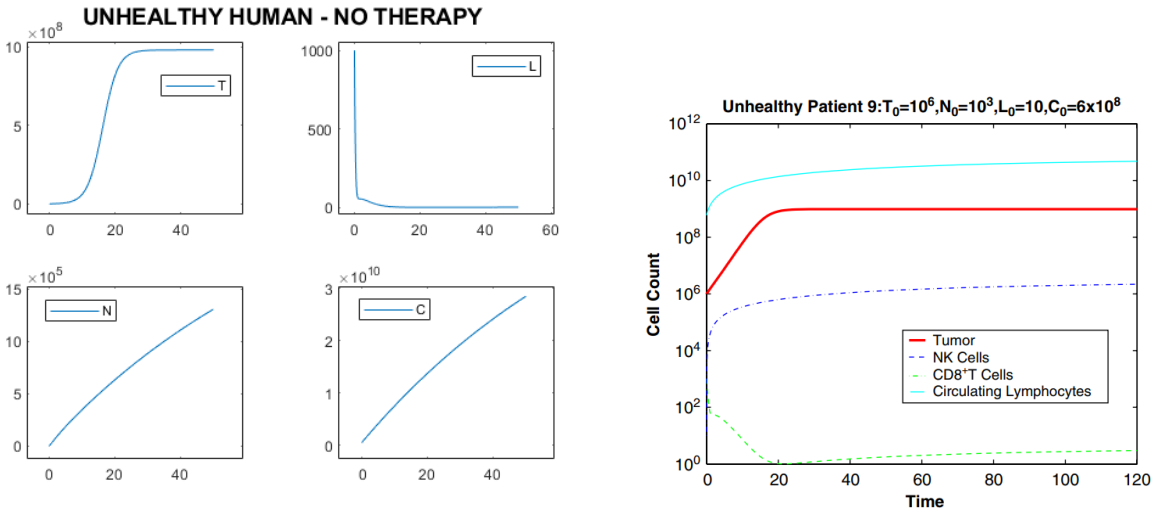

Figure 8: Left: generated in matlab with ode45. Right: figure 7 (right) in the paper. For both: $T_0 = 10^6$; $N_0 = 10^3$; $L_0 = 10$; $C_0 = 6 \times 10^8$. The parameters are the one reported in table 2 in the paper, patient 9.

Chemotherapy

For cases in which the tumor would grow to a dangerous level if left untreated we model pulsed chemotherapy administration into the body, but only after the tumor is large enough to be considered potentially detectable.

The tumor responds differently according to dose pulses. The paper concludes that a tumor of 2×10^7 cells is killed by a dose of $v_M = 5$ per dose for 9 doses over 45 days, as shown in figure 34. In contrast, in our simulations, 5 doses in about 40 days of the $v_M = 3$ are sufficient, as shown in figure 9.

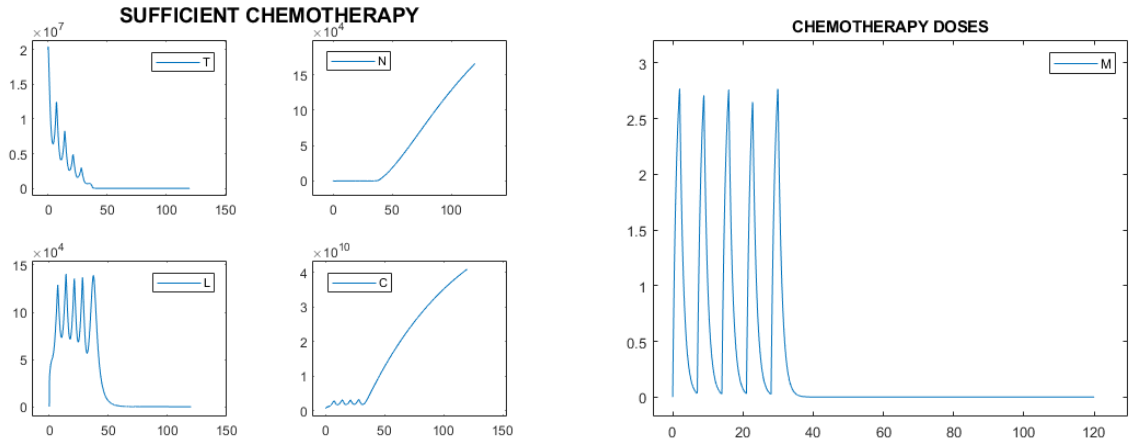

Figure 9: Left: T, R, L, C trend when chemotherapy is administered. Right: progress of chemotherapy administration. $T_0 = 10^6$; $N_0 = 10^3$; $L_0 = 10$; $C_0 = 6 \times 10^8$; $M_0 = 0$. The parameters are the one reported in table 2 in the paper, patient 9. Five chemoterapy doses are administered for every 7 time units of $v_M = 3$ administered over the course of 2 time units.

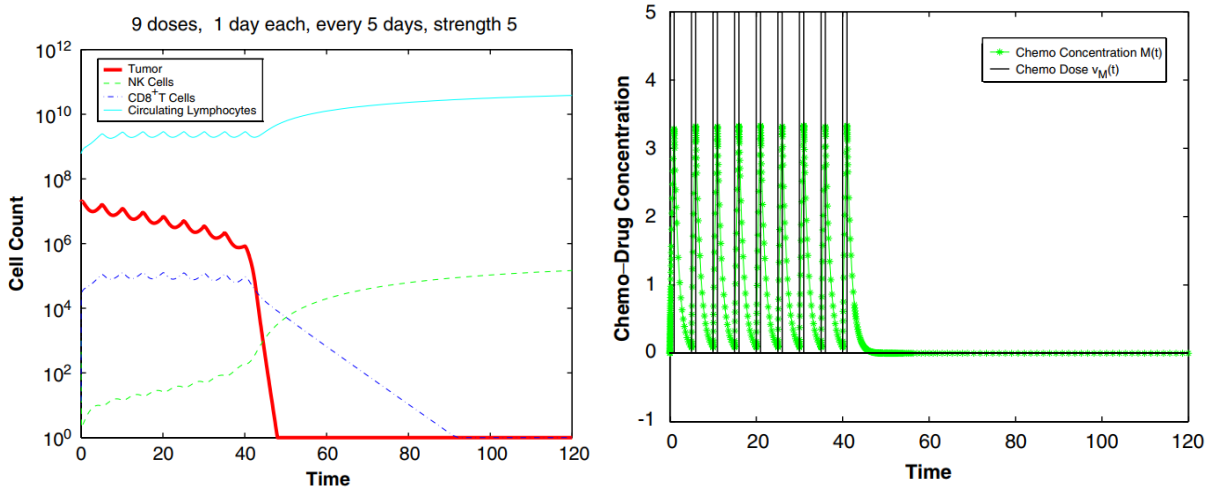

Figure 10: Left: T, R, L, C trend when chemotherapy is administered, took from paper. Right: progress of chemotherapy administration, took from paper. $T_0 = 10^6$; $N_0 = 10^3$; $L_0 = 10$; $C_0 = 6 \times 10^8$; $M_0 = 0$. The parameters are the one reported in table 2 in the paper, patient 9. Nine chemoterapy doses are administered for every 5 time units of $v_M = 5$.

The system is clearly sensitive to the chemotherapy dosing regimen. In the paper, a treatment with the same total chemotherapy, but administered less frequently, once every 10 days will allow the tumor to regrow, as shown in figure 35. Instead, we found that it is sufficient to administer one dose of our dosage every 8 units of time (instead of 7) to allow the tumor to regrow. We also saw that even if the administration is prolonged in time, this is not enough to kill cancer cells.

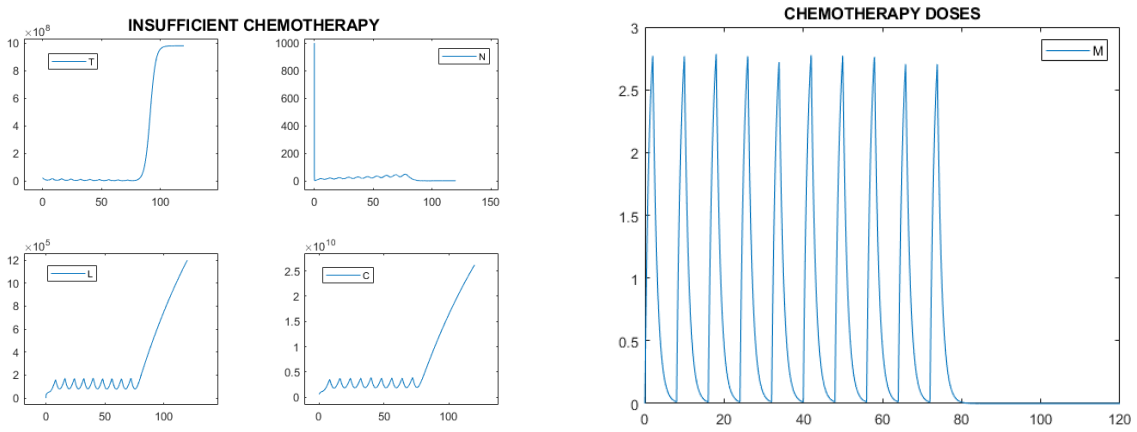

Figure 11: Left: T, R, L, C trend when chemotherapy is administered. Right: progress of chemotherapy administration. $T_0 = 10^6$; $N_0 = 10^3$; $L_0 = 10$; $C_0 = 6 \times 10^8$; $M_0 = 0$. The parameters are the one reported in table 2 in the paper, patient 9. Five chemoterapy doses are administered for every 8 time units of $v_M = 3$ administered over the course of 2 time units.

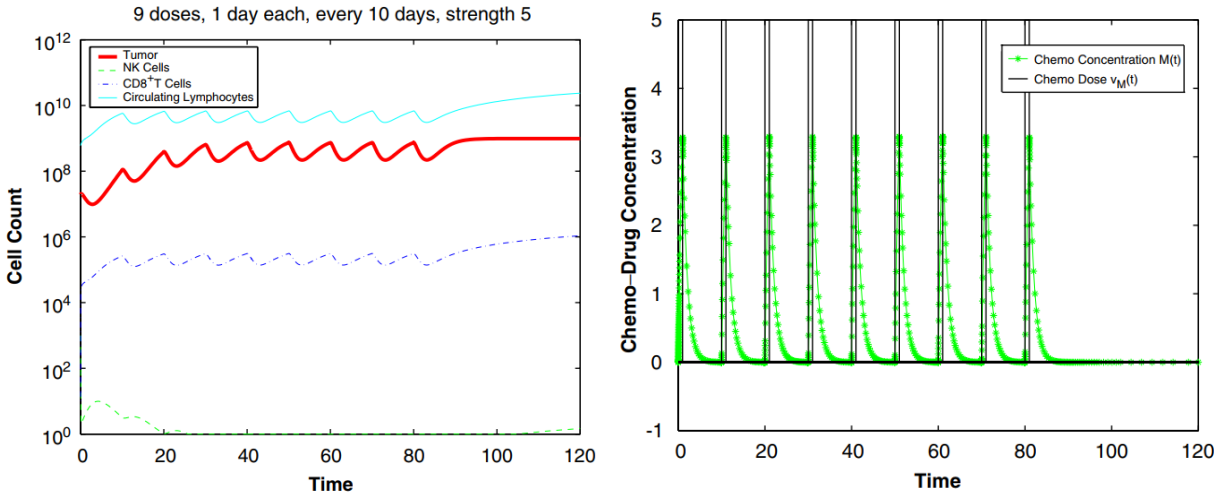

Figure 12: Left: T, R, L, C trend when insufficient chemotherapy is administered, took from paper. Right: progress of chemotherapy administration, took from paper. $T_0 = 10^6$; $N_0 = 10^3$; $L_0 = 10$; $C_0 = 6 \times 10^8$; $M_0 = 0$. The parameters are the one reported in table 2 in the paper, patient 9. Nine chemotherapy doses are administered for every 10 time units, $v_M = 5$.

Immunotherapy

In addition to pure chemotherapy treatments, the paper examines pure immunotherapy treatments. It is investigated immunotherapy in 2 doses of $v_I = 10^9$ and then in 6 doses of 5×10^6 alone against a 10^6 cell tumor (size that immune system cannot control on its own). In this case the paper concludes that immunotherapy succeeds in killing the tumor, as shown in figure 14. In our simulations, we had to shrink the tumor to 3×10^5 cells to achieve the same result, as shown in figure 13. One advantage of this treatment is that the immune system is directly strengthened, and not depleted as it is with chemotherapy, so we see different behaviour in L, N, C from the chemotherapy approach.

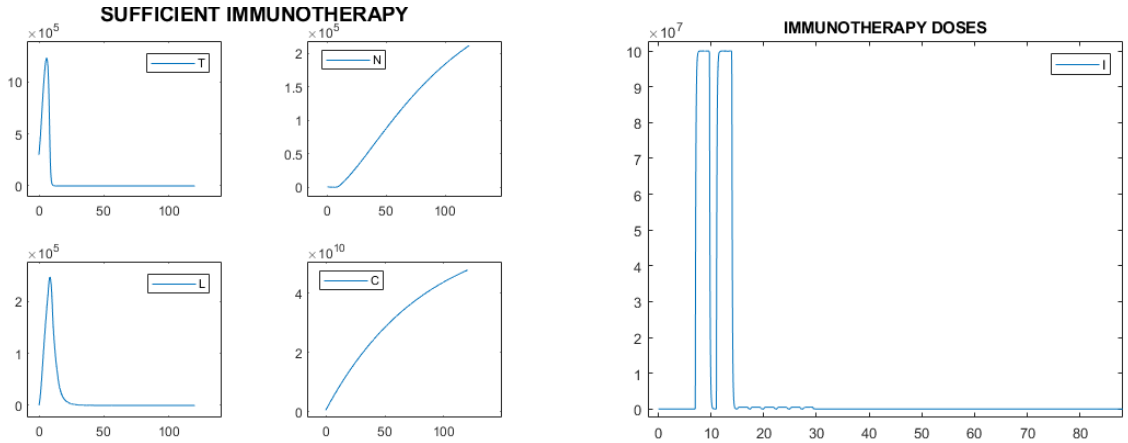

Figure 13: Left: T, R, L, C trend when sufficient immunotherapy is administered. Right: progress of immunotherapy administration. $T_0 = 3 \times 10^5$; $N_0 = 10^3$; $L_0 = 10$; $C_0 = 6 \times 10^8$; $I_0 = 0$. The parameters are the one reported in table 2 in the paper, patient 9. Two immunotherapy doses are administered at the beginning for a duration of 4 time unit, $v_I = 10^9$; immediately afterwards 6 doses of duration 2.5 units of time are administered, $v_I = 5 \times 10^6$.

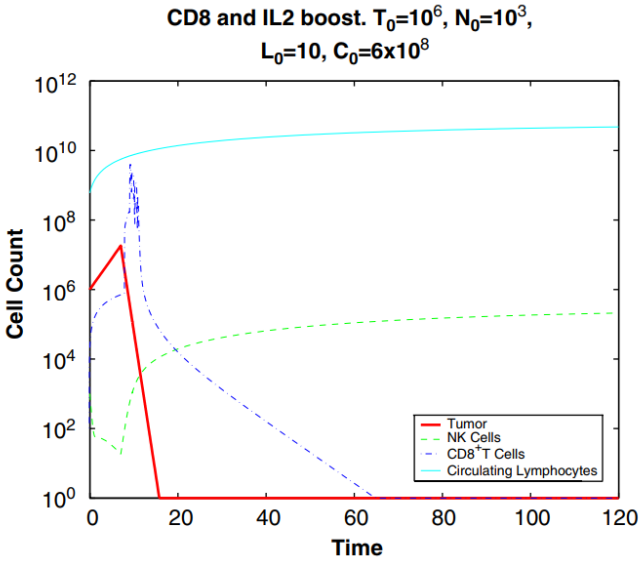

Figure 14: T, R, L, C trend when sufficient immunotherapy is administered, took from paper. $T_0 = 10^6$; $N_0 = 10^3$; $L_0 = 10$; $C_0 = 6 \times 10^8$; $I_0 = 0$. The parameters are the one reported in table 2 in the paper, patient 9. Two immunotherapy doses are administered at the beginning, $v_I = 10^9$; afterwards 6 doses of $v_I = 5 \times 10^6$ are administered.

From our result it is straightforward to deduce that effectiveness may be limited to smaller tumor sizes. In fact, both in the paper and from our simulations we get that with a little larger tumor, immunotherapy is not sufficient to kill the tumor. The paper obtains that with a tumor of 10^7 cells and the same previous conditions, immunotherapy is not sufficient, as shown in figure 16. We get the same result with a tumor of 5×10^5 cells, as shown in figure 15.

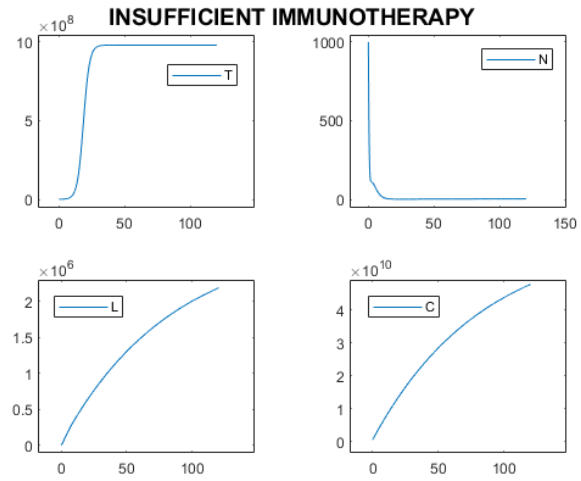

Figure 15: T, R, L, C trend when insufficient immunotherapy is administered. $T_0 = 5 \times 10^5$; $N_0 = 10^3$; $L_0 = 10$; $C_0 = 6 \times 10^8$; $I_0 = 0$. The parameters are the one reported in table 2 in the paper, patient 9. Two immunotherapy doses are administered at the beginning, $v_I = 10^9$; afterwards 6 doses of $v_I = 5 \times 10^6$ are administered.

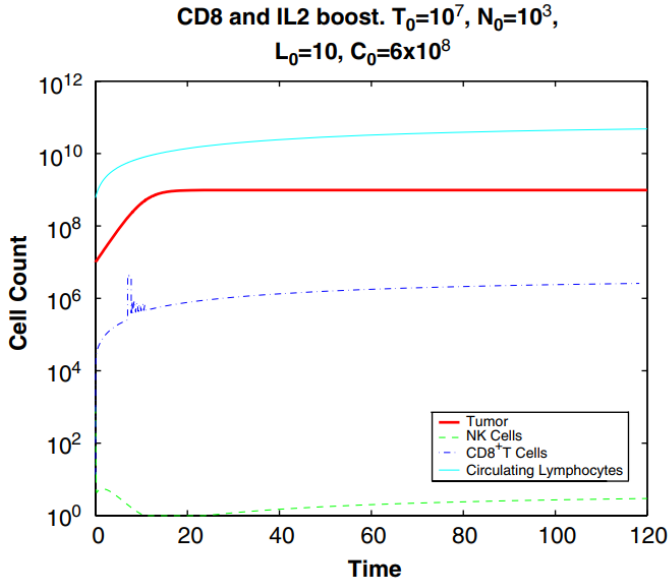

Figure 16: T, R, L, C trend when sufficient immunotherapy is administered, took from paper. $T_0 = 10^7$; $N_0 = 10^3$; $L_0 = 10$; $C_0 = 6 \times 10^8$; $I_0 = 0$. The parameters are the one reported in table 2 in the paper, patient 9. Two immunotherapy doses are administered at the beginning, $v_I = 10^9$; afterwards 6 doses of $v_I = 5 \times 10^6$ are administered.

Combination therapy

We have presented cases for which chemotherapy alone or immunotherapy alone cannot kill a tumor. In the paper, subsequent attempts are made to combine the two therapies to kill these types of tumors. In the paper one criterion used is to measure the health of the patient as a function of the number of circulating lymphocytes, kept above 10^8 cells (otherwise we incur risk of infection). Again in our simulations there will be modifications to the initial parameters and you will get vaguely different results, but we also managed not to go below the threshold.

The paper shows that for the case in figure 37 a combination treatment is now able to eliminate a tumor of 10^7 cells, which previously immunotherapy alone failed to destroy (figure 16, the same initial data are used). Combination therapy, as seen from the right side of the figure 37, consists of an administration of chemotherapy and immunotherapy. This allows less chemotherapy (which causes damage to the body) to be administered while keeping immune cell counts high. This therapy is also tested in the paper for larger tumors, but it fails unless different dosages and periods of administration of both chemotherapy and immunotherapy are adopted (no pictures of these experiments are reported in paper).

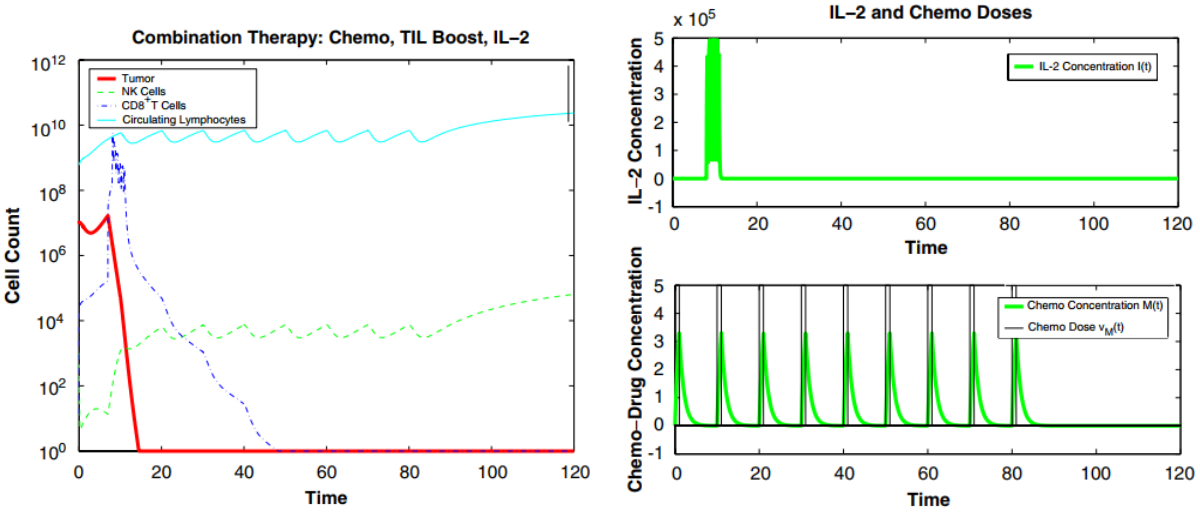

Figure 17: Left: T, R, L, C trend when sufficient combination therapy is administered, took from paper. Right: progress of chemotherapy and immunotherapy administration, took from paper. $T_0 = 2 \times 10^7$; $N_0 = 10^3$; $L_0 = 10$; $C_0 = 6 \times 10^8$; $I_0 = 0$; $M_0 = 0$. The parameters are the one reported in table 2 in the paper, patient 9. Two immunotherapy doses are administered in 2 time unit, $v_I = 10^9$, then six immunotherapy doses are administered during 4 time unit, $v_I = 5 \times 10^5$. Nine chemotherapy doses are administered once every 10 days for a duration of 1 time unit, $v_M = 5$.

We obtained similar results by lowering the intensity of immunotherapy and the number of doses administered of both therapies, as shown in figure 18.

However, it is enough for a patient to have a compromised immune system for combination therapy to be less effective, as shown in figure 38 for a different patient. We also obtained similar results in figure 20.

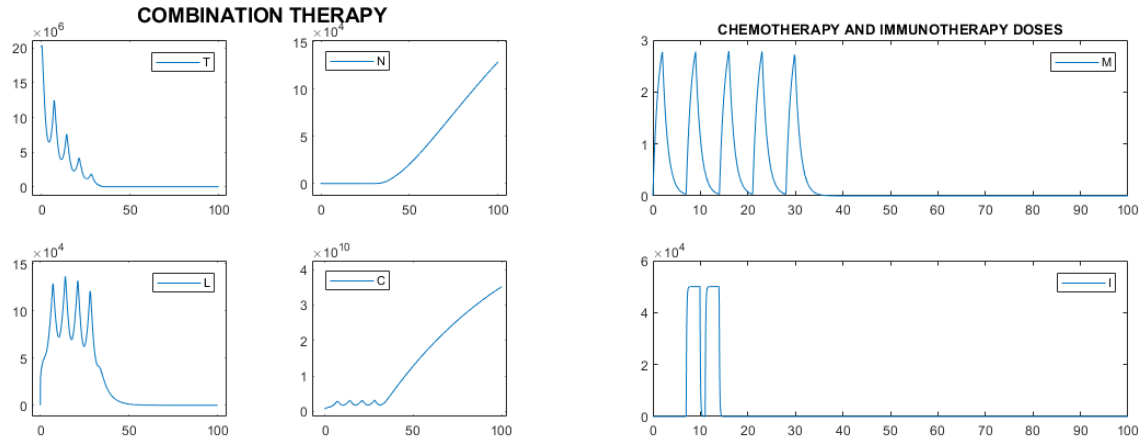

Figure 18: Left: T, R, L, C trend when sufficient combination therapy is administered. Right: progress of chemotherapy and immunotherapy administration. $T_0 = 2 \times 10^7$; $N_0 = 10^3$; $L_0 = 10$; $C_0 = 6 \times 10^8$; $I_0 = 0$; $M_0 = 0$. The parameters are the one reported in table 2 in the paper, patient 9. Two immunotherapy doses are administered at the beginning for a duration of 4 time unit, $v_I = 5 \times 10^5$. Five chemotherapy doses are administered for a duration of 7 time unit, $v_M = 3$.

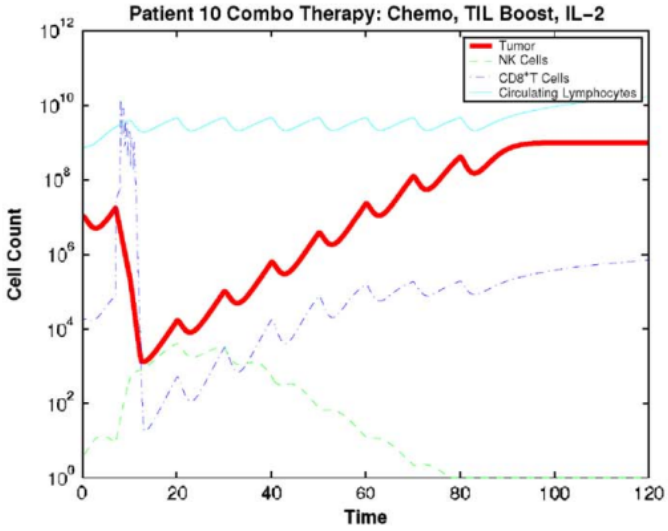

Figure 19: T, R, L, C trend when insufficient combination therapy is administered, took from paper. $T_0 = 10^7$; $N_0 = 10^3$; $L_0 = 10$; $C_0 = 6 \times 10^8$; $I_0 = 0$; $M_0 = 0$. The parameters are the one reported in table 2 in the paper, patient 10 with compromised immune system. Two immunotherapy doses are administered in 2 time unit, $v_I = 10^9$, then six immunotherapy doses are administered during 4 time unit, $v_I = 5 \times 10^6$. Nine chemotherapy doses are administered once every 10 days for a duration of 1 time unit, $v_M = 5$.

However, it is possible even in this immune-compromised patient to achieve a positive outcome, provided that the chemotherapy dosage and immunotherapy administrations are prolonged, as is shown in the paper.[3]

[3]We could not simulate the same result because it is necessary to precisely combine immunotherapy with chemotherapy so that the negative effects of the latter on immune cells are tamed. As previously mentioned, the data used in the paper do not provide the same results for us.

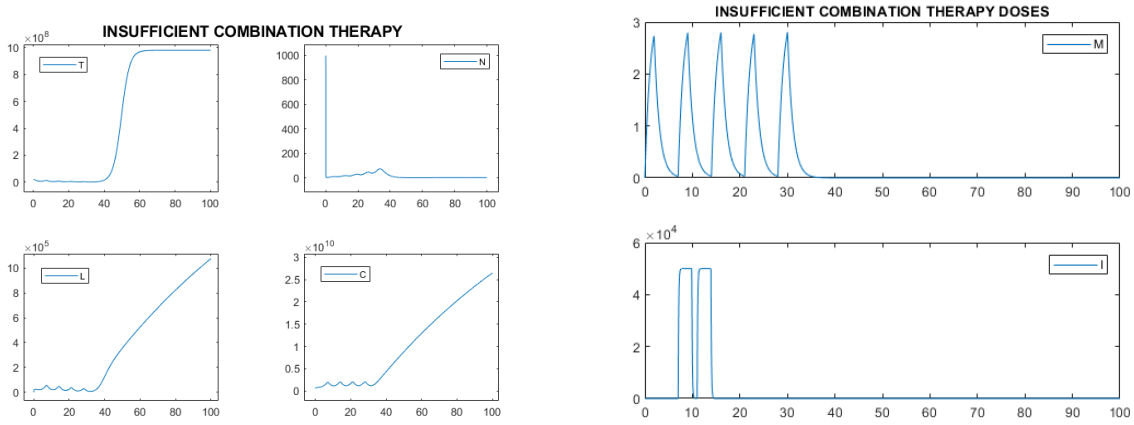

Figure 20: Left: T, R, L, C trend when insufficient combination therapy is administered. Right: progress of chemotherapy and immunotherapy administration. $T_0 = 2 \times 10^7$; $N_0 = 10^3$; $L_0 = 10$; $C_0 = 6 \times 10^8$; $I_0 = 0$; $M_0 = 0$. The parameters are the one reported in table 2 in the paper, patient 10 with compromised immune system. Two immunotherapy doses are administered at the beginning for a duration of 4 time unit, $v_I = 5 \times 10^5$. Five chemotherapy doses are administered for a duration of 7 time unit, $v_M = 3$.

Vaccine therapy

In addition to chemotherapy and immunotherapy, in the paper is also simulated the cancer vaccine, which is a special case of immunotherapy for treating cancer. As with all vaccine, the body is challenged with some modified form of the cancer, consequently sensitizing the immune system to the presence of the cancer, allowing the immune system more effectively to find and lyse cancer cells. In order to simulate vaccine therapy for human patients, it is necessary to change the values of five parameters at the time of vaccination (documented by experimental data, see the paper for references): c, the fractional tumor cell kill by natural killer cells, g, the maximum NK-cell recruitment rate by tumor cells, j, the maximum $CD8^+T$ cell recruitment rate, s, the steepness coefficient of the tumor–$CD8^+T$ competition term, d, the saturation level of fractional tumor cell kill by $CD8^+T$ cells, and l, the exponent of fractional tumor cell kill by $CD8^+T$ cells. Values of c, g, j, d were increased, value of s is decreased (value of l was not changed).

First case analysed is a theoretical case in which a patient has a tumor of size 2×10^7 and a "healthy" immune system of 3×10^5 NK cells, 10^2 $CD8^+T$ cells, and 10^{10} circulating lymphocytes (not sufficient to kill the tumor alone, not shown in the paper).

As shown in figure 39 (left), the body cannot handle this size tumor when aggressive chemotherapy is administered for 50 days. Additionally, as shown in figure 39 (center), vaccine therapy, represented by changes to the parameters after 10 days, fails to kill the tumor. Only the combination of both treatments can kill a tumor of this magnitude, as shown in figure 39 (right). Such dramatic tumor regression is still uncommon among most patients, and sensitive to the choice of tumor and patient parameters, as well as to the timing of the treatments.

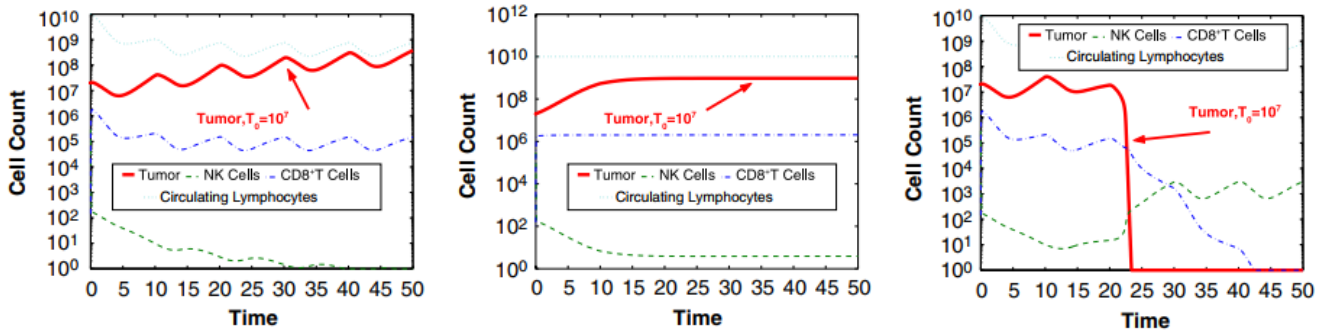

Figure 21: T, R, L, C trend in different therapy, took from paper. $T_0 = 2 \times 10^7$; $N_0 = 3 \times 10^5$; $L_0 = 100$; $C_0 = 10^{10}$. Left: $v_M = 2$ administered for 3 consecutive days every 10 days. Center: vaccine is administered at day 10, $c = 7.131 \times 10^{-9}$; $g = 0.5$; $j = 1$; $s = 0,0019$; $d = 15$. Right: combination of the two previous therapies. For all three cases the parameters are the one reported in table 2 in the paper, patient 9.

In our simulations, as shown in figure 22, we obtained similar results with the difference of a higher dose of chemotherapy: $v_M = 3.4$. The descent of tumor cell number is perhaps less steep than in the paper, but the

conclusions are the same.

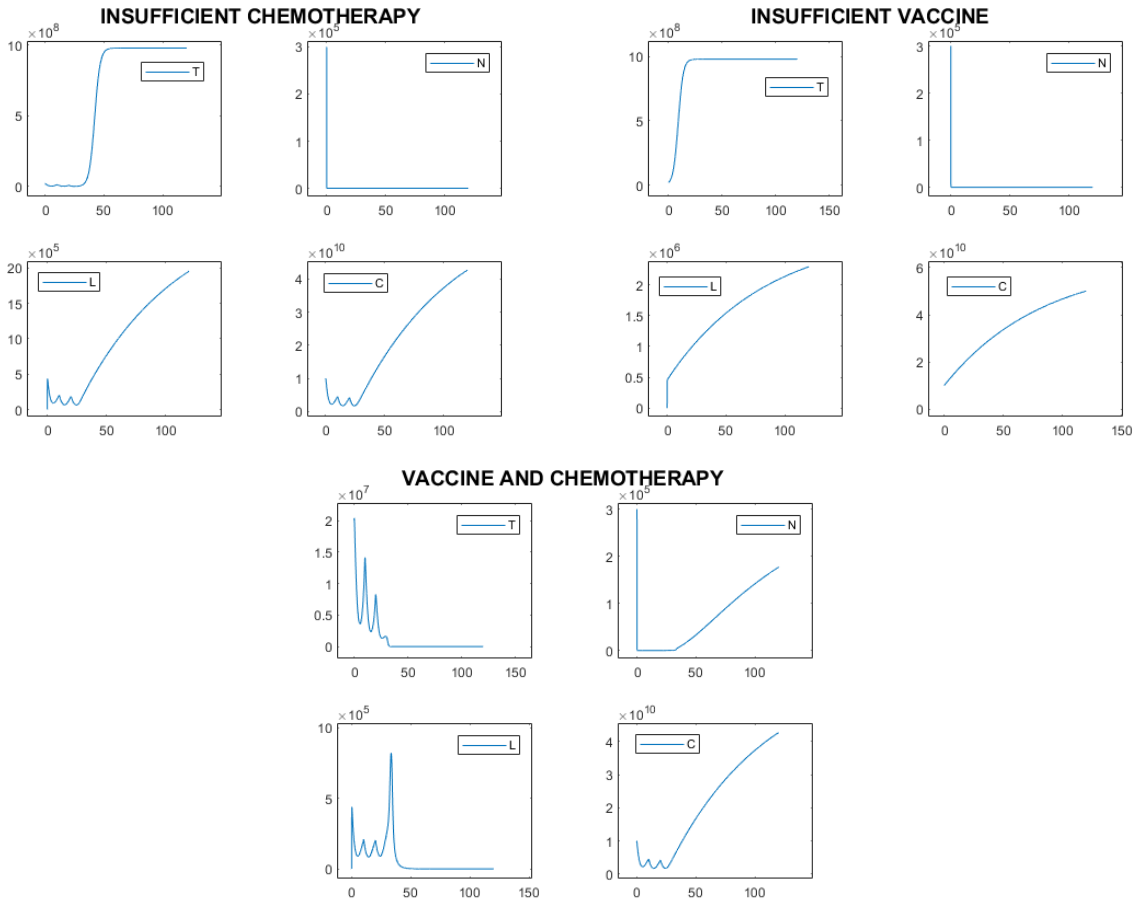

Figure 22: T, R, L, C trend in different therapy. $T_0 = 2 \times 10^7$; $N_0 = 3 \times 10^5$; $L_0 = 100$; $C_0 = 10^{10}$. Top left: $v_M = 3.4$ administered for 3 time units every 10 time units. Top right: vaccine is administered at time unit 10, $c = 7.131 \times 10^{-9}$; $g = 0.5$; $j = 1$; $s = 0,0019$; $d = 15$. Bottom: combination of the two previous therapies. For all three cases the parameters are the one reported in table 2 in the paper, patient 9.

There are cases for which vaccine therapy alone is able to control a growing tumor, but the simulations in paper indicate that timing is an important factor in determining the effectiveness of the vaccine treatment. For as it was modeled in the paper, i.e. as a change in parameters, and not as a drug population, the amount of vaccine cannot be altered, but the timing of administration can be controlled.

In the paper is simulated the case of an initial tumor is set to be 10^7 cells (half the size of the previous experiment), and same immune system initial conditions. In this case the vaccine therapy alone effectively eliminates the tumor when administered the 13th day. If administered any later, it is ineffective, as is shown in figure 40.
We were not able to obtain the same result with the same data.

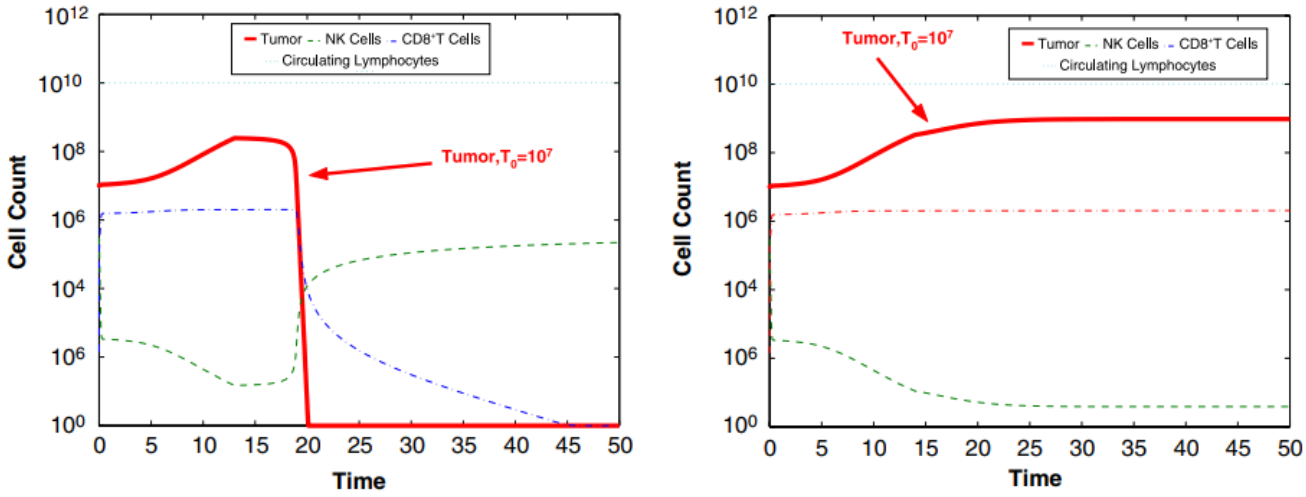

Figure 23: T, R, L, C trend in different therapy, took from paper. $T_0 = 10^7$; $N_0 = 3 \times 10^5$; $L_0 = 100$; $C_0 = 10^{10}$. Left: vaccine is administered at day 13. Right: vaccine is administered at day 14. In both cases the vaccine is modeled as: $c = 7.131 \times 10^{-9}$; $g = 0.5$; $j = 1$; $s = 0,0019$; $d = 15$. The other parameters are the one reported in table 2 in the paper, patient 9.

2 Coletti's model

The second examined model regards the effect of immunotherapy for castration-resistant prostate cancer. Since this type of tumor develops in an androgen sensitive form (ADPC), patients are often treated with androgen deprivation therapy. In some cases, though, the cancer cells may change into a castration-resistant form (AIPC). Coletti's paper mainly focuses on the latter manifestation and in particularly examines the following three treatments: *androgen deprivation therapy*, *dendritic vaccine sipuleucel-T* and *ipilimumab*, an immune checkpoint blockade drug targeting Cytotoxic T-Lymphocyte Antigen 4 (CTLA4), exposed on the CTLs membrane.

Assumption

This model extends the one presented by *Rutter and Kuang* (2017) with immunotherapy: ipilimumab drug, an anti-CTLA4 treatment, has been added and the presence of immune-suppressive tumor-microenviroment description by Treg cells has been considered as well. Since the purpose of this report is to examine the mathematical aspects of the model, we will not go into the biological details, but the main assumptions will be mentioned. In particular, two important hypotheses are that tumor proliferation is presumed logistic and the inactivation process by Treg is supposed to follow a mass action law.

Model equation

The model describes the evolution in time of the following variables:

- $X_1(t)$ Androgen Dependent Prostate Cancer cells (ADPC)
- $X_2(t)$ Androgen Independent Prostate Cancer cells (AIPC)
- $C(t)$ circulating Cytotoxic T Lymphocytes (CTL)
- $R(t)$ circulating Treg cells (Treg)
- $I_L(t)$ interleukin-2 in blood
- $D(t)$ circulating Dendritic cells
- $A(t)$ Androgen concentration
- $I_P(t)$ Ipilimumab drug

The equations governing the variables kinetics take into account the following interactions (see figure 24):

- $ADPC$ is positively influenced by A, while, in the case of *androgen deprivation therapy*, $ADPC$ could be transformed into $AIPC$
- CTL, which attacks both the two type of cancer cells, is down-regulated by $Treg$
- I_L positively influences CTL and $Treg$
- D ($vaccine$) is the principal stimulus for CTL
- I_P ($anti\text{-}CTLA4$) interacts with the CTL increasing its capacity to kill $ADPC$ and $AIPC$

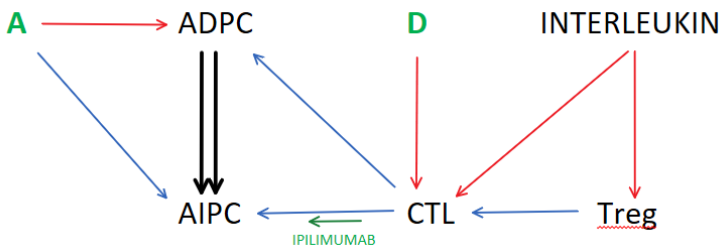

Figure 24: Biological interactions between some variables (in black) and treatments (in green) where red arrows indicate positive influence while blue ones represent inhibition

On the whole, the model that has been constructed has the following structure:

$$\frac{dX_1}{dt} = \overbrace{r_1\, A\, X_1\left(1-\frac{X_1+X_2}{K}\right)}^{Tumor\ proliferation} - \overbrace{\mu_1\left(1-\frac{A}{a_0}\right)X_1}^{Death} - \overbrace{m_1\left(1-\frac{A}{a_0}\right)X_1}^{Mutation} - \overbrace{C\, X_1\left(\frac{e_{CX}}{g_{CX}+(X_1+X_2)}+k_{lp}\, I_P\right)}^{CTL\ effect}$$

$$\frac{dX_2}{dt} = \overbrace{r_2\, X_2\left(1-\frac{X_1+X_2}{K}\right)}^{Tumor\ proliferation} + \overbrace{m_1\left(1-\frac{A}{a_0}\right)X_1}^{Mutation} - \overbrace{C\, X_2\left(\frac{e_{CX}}{g_{CX}+(X_1+X_2)}+k_{lp}\, I_P\right)}^{CTL\ effect}$$

$$\frac{dC}{dt} = \overbrace{e_C\,\frac{D}{g_C+D}}^{Activation\ by\ D} + \overbrace{\frac{e_{IC}\, C\, I_L}{g_{IC}+I_L}}^{I_L\ effect} - \overbrace{\mu_C\, C}^{Death} - \overbrace{k_R\, C\, R}^{T_{reg}\ effect}$$

$$\frac{dR}{dt} = \overbrace{a_R\, D}^{D\ effect} - \overbrace{\mu_R\, R}^{Death} + \overbrace{a_{IR}\, I_L}^{I_L\ effect}$$

$$\frac{dD}{dt} = \overbrace{s_D}^{Source} - \overbrace{\mu_D\, D}^{Death} + \overbrace{v}^{Vaccine}$$

$$\frac{dI_L}{dt} = \overbrace{e_I\frac{C\,(X_1+X_2)}{g_I+(X_1+X_2)}}^{Tumor's\ and\ CTL's\ effect} + \overbrace{\mu_I(i_0-I_L)}^{Proliferation\ and\ death}$$

$$\frac{dA}{dt} = \overbrace{\gamma_A(a_0-A)}^{Proliferation\ and\ death} - \overbrace{\gamma_A\, a_0\, \mathbf{1}_{CX}}^{Tumor's\ and\ CTL's\ effect}$$

$$\frac{dI_p}{dt} = -\overbrace{\gamma_p\, I_p}^{ICB\ degradation}$$

The equations in the model have been scouted also analysing the effect that each possible treatment causes.

In the first one, the rate at which X_1 changes strictly depends on the level of androgen, where a_0 is its basal level. Considering untreated cases, the death term is exactly zero and tumor dies only if CTL killing rate is effective enough. On the other hand, if we consider androgen deprivation treatment, X_1 proliferation decreases while its death rate increases. The main problem of this therapy is that, due to selective pressure, mutation term increases as well, thus $ADPC$ would rapidly transform into $AIPC$. Moreover, CTL's effect is composed of two terms, the first one describes tumor ability to bypass the immune system, while the second one reflects the effects of $ICBs$ treatments.

The second equation has analogous terms respect to the aforementioned one but with a main difference: its proliferation rate does not depend on the androgen level, hence it is not effected by the androgen deprivation therapy. Regarding the third equation, it is important to notice how dendritic cells activate CTL and how I_L has a positive effect on it. On the other hand, Treg have a negative impact on the immune system's enhancement against tumor cells.

The fourth and fifth equations deal with R and D rates, in particularly, the second one depends on the vaccine therapy, simulated as a constant infusion, and both of the two derivatives depend also on D. Concerning I_L, A and I_p, proliferation, death and drugs degradation have been taken into account as shown in the model. Specifically, androgen deprivation effect has been modeled as a boolean function (equal to 1 if the treatment is considered, to zero otherwise), and I_p administrations are considered to be instantaneously increased of a fixed constant.

Furthermore, through the equation

$$PSA(t) \;=\; c_{PSA}\,(X_1(t)+X_2(t)),$$

it is possible to understand how the evolution of tumor cells changes *Prostate Specific Antigene*(PSA), whose high level is often associated with prostate cancer.

Parameters value

Every parameter of the model has been estimated as shown in Appendix A of Coletti's paper, these values are used in Matlab analysis to implement the code and to study the dynamics of the solutions.

Numerical experiment

Coletti's model could be used to simulate different scenario and to try to predict which is the outcome for each treatment or combined therapy. The simulations have been carried out over a 7-years period of time in order to be able to

examine the short term dynamics as well as the long term ones.

First, it is possible to study which is the behaviour of the model in case of no drugs nor other therapies have been taken to deal with the tumor. Indeed, in order to run this simulation, the parameters have been set to $v = 0$, $I_{CX} = 0$ and $I_P(0) = 0$ and their results are shown in figure 25. As expected, ADPC cancer cells increase, until reaching a constant threshold value. Simultaneously, PSA reaches its maximum level while there is no AIPC creation since there is no pressure into the androgen-independent cancer form.

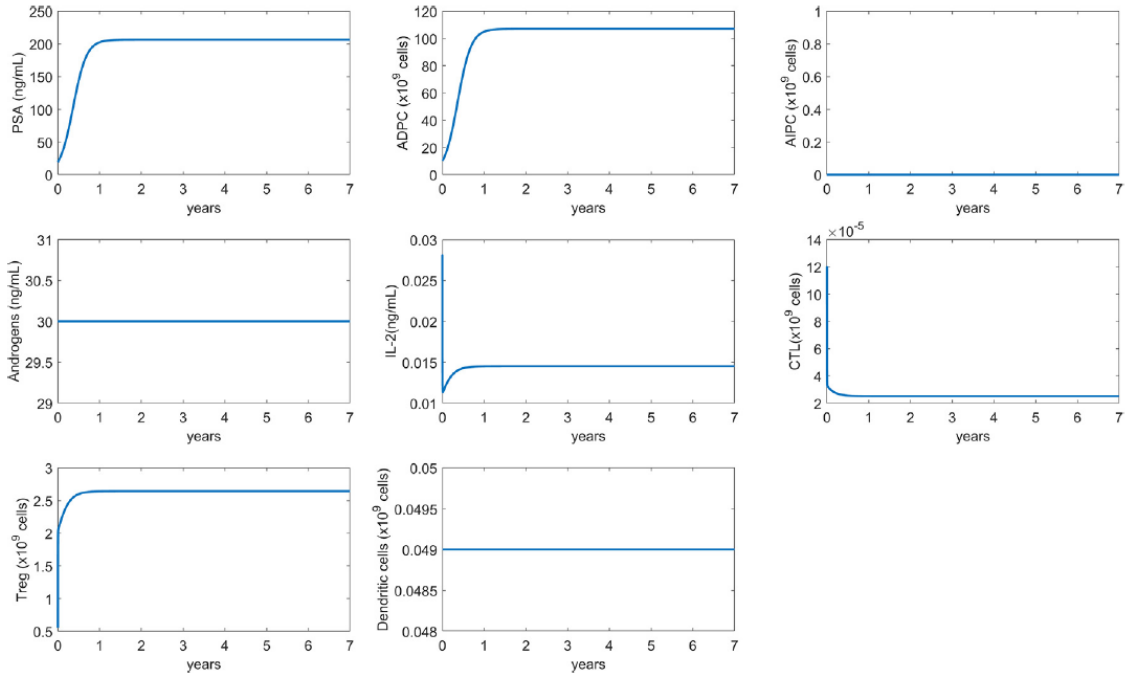

Figure 25: Simulation: untreated case

Another experiment, which simulates the androgen deprivation treatment by itself or combined with dendritic cells vaccine, has been analysed in figure 26. In this case, PSA level first decreases due to the destruction of ADPC, but it secondly starts increasing again due to the selection of androgen independent cancer form. Combining the therapy with the vaccine does not change much the outcome of the simulation. Indeed, even if dendritic cells injection helps the immune system to increase CTL and Treg values, the variables PSA, ADPC and AIPC do not show any relevant differences compared to the above case and the result is still the spread of the cancer.

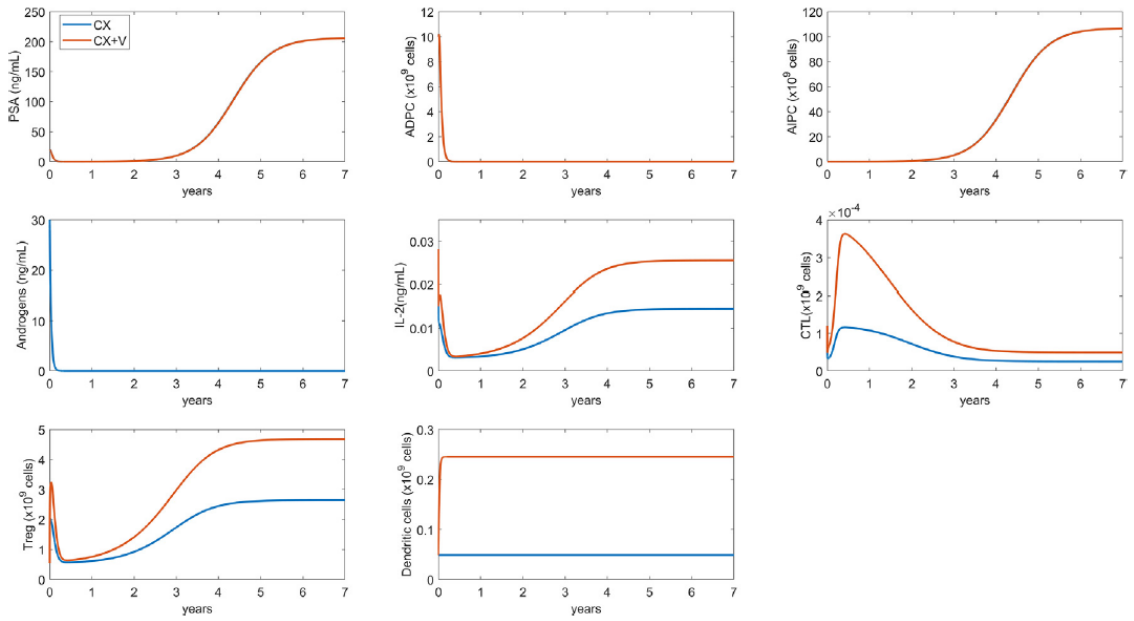

Figure 26: Simulation: androgen deprivation therapy by itself (blue) and combined with the vaccine treatment (orange)

Regarding Anti-CTLA4 treatment, results are different depending on the schedules and the doses of the drug. Figure 27 displays the differences in the dynamic of the model with three distinct values over a one-year period of time. Again, due to the androgen deprivation therapy, ADPC are destroyed while AIPC are selected. Subsequentely, no matter of the AntiCTLA4 drug dose, PSA level will start to increase again and the high-tumor level will be reached soon or later.

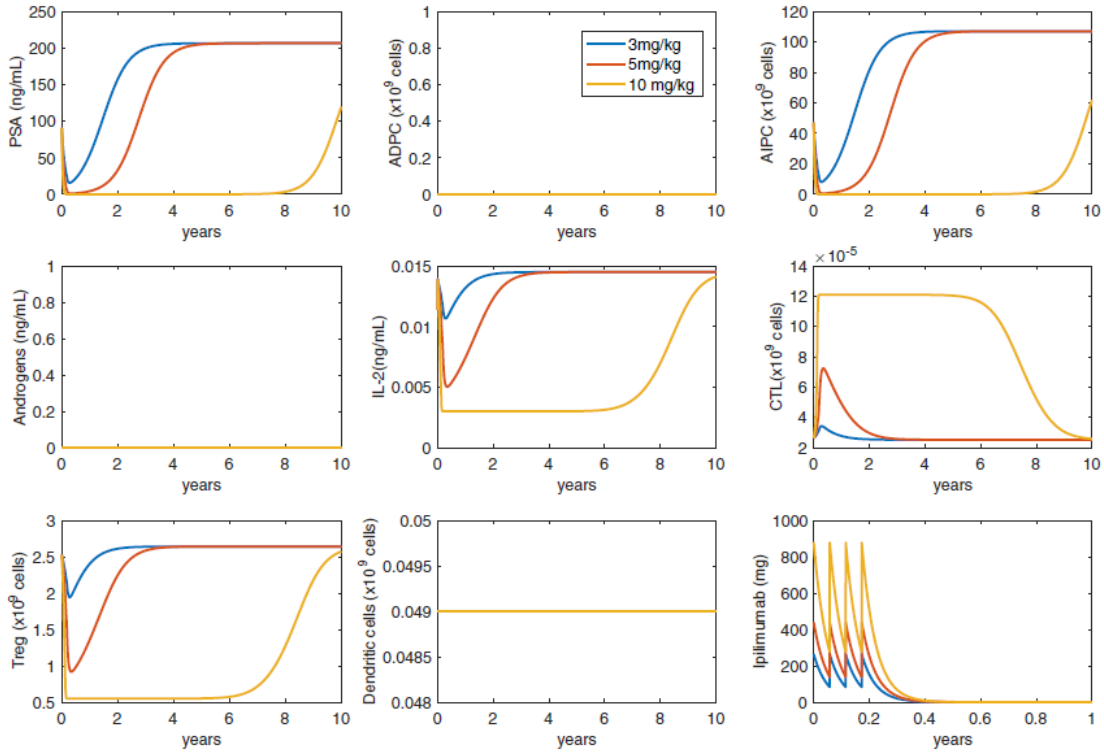

Figure 27: Simulation: androgen deprivation therapy combined with intermittent ipilimumab injection in different doses

Choosing a repeated intermittent treatment with a low dose returns better simulations results. Looking at figure 28, it is clear that, once ADPC is eradicated, PSA and AIPC levels will keep oscillating with lower and lower peaks, while the response of the immune system in terms of CTL cells gets stronger. Anyway, this still is not enough to eradicate the cancer since increasing the simulation time the system restarts going towards a high-tumor level. This seams to show that, even with this administration schedule, the no-tumor point is not an attractive equilibria and the

tumor will not get eradicated.

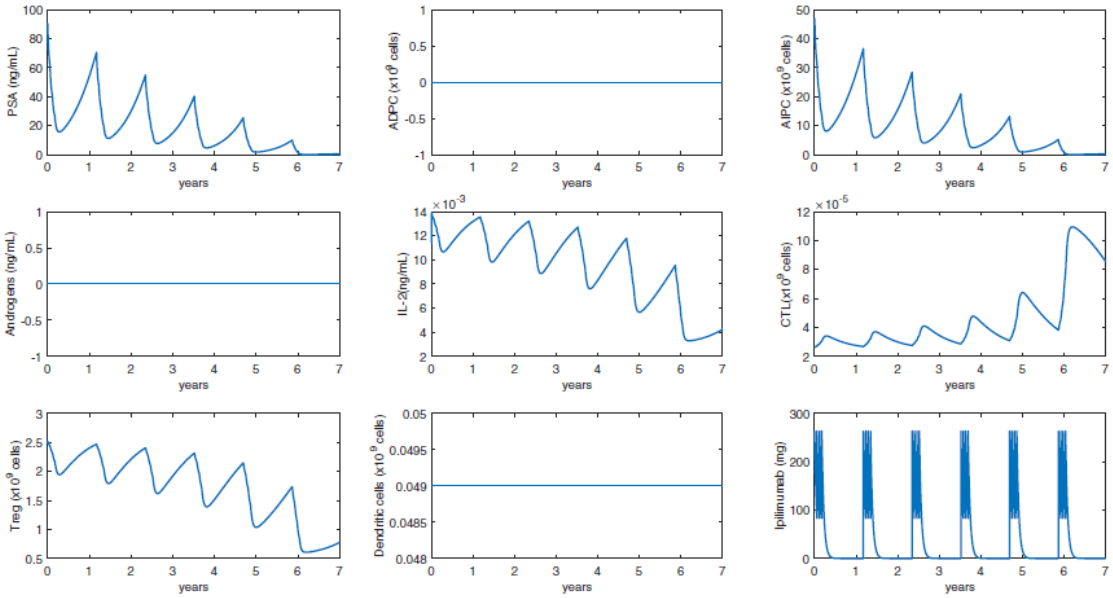

Figure 28: Simulation: androgen deprivation therapy combined with repeated intermittent ipilimumab injections

Finally, the last simulation has been run under the hypothesis of an early administered treatment with repeated and intermittent ipilimumab injections in combination with androgen deprivation therapy. The plots in figure 29 exhibit a better tumor control where, as the therapy starts, ADPC suddenly disappear and AIPC's value oscillates tending to the no-tumor point.

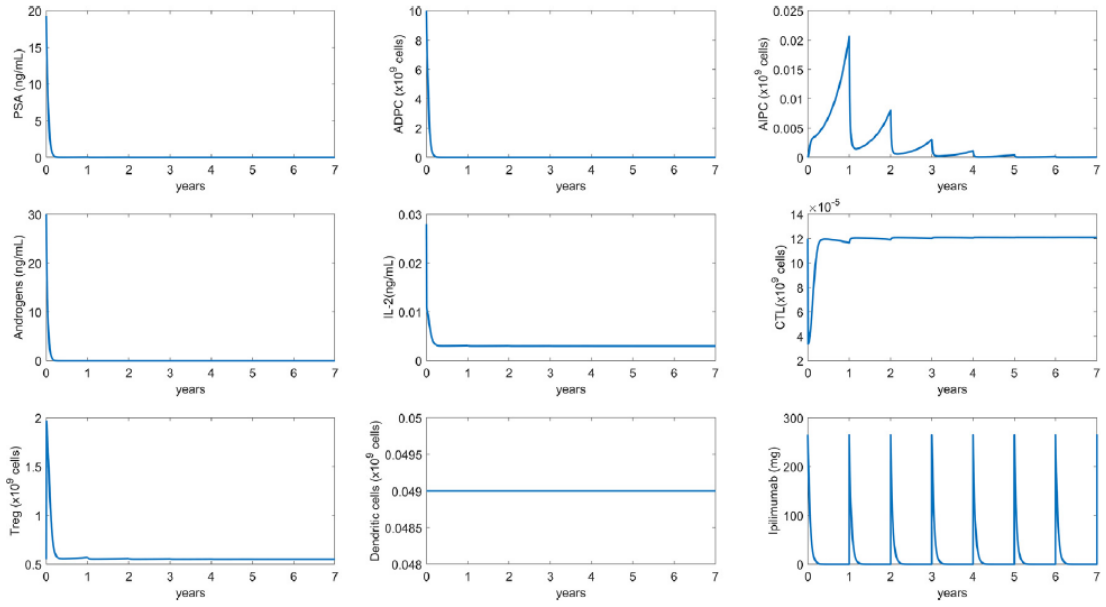

Figure 29: Simulation: androgen deprivation therapy combined with early administered and repeated intermittent ipilimumab injections

Model reduction

In order to simplify the model and thus to be able to properly study its solutions, we further assume that I_p is administered with a constant rate following a long-term therapy and we consider androgen deprivation as the main treatment. Thus the 8^{th} and 9^{th} equations of the model have been changed into:

$$\frac{dA}{dt} = -\gamma_a\, A, \qquad \frac{dI_p}{dt} = d_p - \lambda_p\, I_p.$$

Moreover, it can be observed that D, I_L, I_p and A vary in shorter time scales than the other variables thus, using the quasi-steady approach, these variable are assumed to be equal to

$$A^* = 0, \qquad D^* = \frac{s_D + v}{\mu_D}, \qquad I_p^* = \frac{d_p}{\lambda_p}, \qquad I_L(C, X_1, X_2) = i_0 + \frac{e_I\ C\ (X_1 + X_2)}{\mu_I(g_I + X_1 + X_2)}.$$

To further simplify the structure of the model, source terms have also been introduced as $s_R = a_R\ D^*$ and $s_C = e_C\ \frac{D^*}{g_C + D^*}$.

Finally, since it is known that $\frac{dX_1}{dt} < 0$ and $\lim_{t\to+\infty} X_1(t) = 0$, we can considered the following limiting system:

$$\begin{aligned}
\frac{dX_2}{dt} &= r_2\ X_2 \left(1 - \frac{X_2}{K}\right) - C\ X_2 \frac{e_{CX}}{g_{CX} + X_2} + C\ X_2\ k_{lp}\ I_P^*; \\
\frac{dC}{dt} &= s_C + \frac{e_{IC}\ C\ I_L(C, 0, X_2)}{g_{IC} + I_L(C, 0, X_2)}\ - \mu_C\ C - k_R\ C\ R; \\
\frac{dR}{dt} &= s_R - \mu_R\ R + a_{IR}\ I_L(C, 0, X_2).
\end{aligned}$$

Equilibria

In order to look for the equilibria of the limiting system, we need to find the zeros of the equations.
Thus, if we set $X_2^o = 0$, hence no tumor is present and $I_L(C, 0, 0) = i_0$, we obtain

$$\begin{aligned}
X_2^o &= 0; \\
C^o &= \frac{s_C}{\mu_C\ k_R\ R^0 - \frac{e_{IC}\ i_0}{g_{IC} + i_0}}; \\
R^o &= \frac{s_R + a_{IR}\ i_0}{\mu_R}.
\end{aligned}$$

Therefore, even without any treatment, there exists $E^o = (X_2^o, C^o, R^o)$, a *no-tumor equilibria*, if $\mu_C\ k_R\ R^0 > \dfrac{e_{IC}\ i_0}{g_{IC} + i_0}$.

The aim now is to understand which type of stability this point has and whether there are other equilibrium involved. Numerical simulations will show this is the case.

Stability

The Jacobian matrix of the limiting system evaluated in E^o is

$$J(E^o) = \begin{pmatrix} r_2\ - C^o\ \frac{e_{CX}}{g_{CX}} & 0 & 0 \\ \dots & \frac{e_{IC}\ i_0}{g_{IC} + i_0} - \mu_C - k_R\ R & -k_R C^o \\ \dots & 0 & -\mu_R \end{pmatrix}.$$

Thus, the characteristic polynomial of the matrix is

$$p(\lambda) = -\left(r_2\ - C^o\ \frac{e_{CX}}{g_{CX}} - \lambda\right)\left(\frac{e_{IC}\ i_0}{g_{IC} + i_0} - \mu_C - k_R\ R^o - \lambda\right)(\mu_R + \lambda)$$

and its roots are

$$\begin{aligned}
\lambda_1 &= r_2\ - C^o\ \frac{e_{CX}}{g_{CX}}; \\
\lambda_2 &= \frac{e_{IC}\ i_0}{g_{IC} + i_0} - \mu_C - k_R\ R^o; \\
\lambda_3 &= -\mu_R.
\end{aligned}$$

Given that $\lambda_2 < 0$ and $\lambda_3 < 0$, E^o is stable if and only if $\lambda_1 < 0$, hence if and only if

$$r_2 < C^o\ \frac{e_{CX}}{g_{CX}}.$$

Therefore, under this model assumption and in order to be able to approach the no-tumor equilibrium and completely remove the cancer cells, it is necessary that the rate of proliferation of AIPC is lower than the CTL killing capacity. Taking r_2 as a bifurcation parameter, the critical threshold is $r_{BP}^o = C^o\ \frac{e_{CX}}{g_{CX}}$ which is associated to a transcritical bifurcation (see Appendix B of Coletti's paper).

If we consider the *vaccine therapy*, the patient is submitted to what can be assumed to be a constant injection of dendritic cells, which activate CTL, thus C^o significantly increases. All of this brings to the growth of the threshold r_{BP}.

Regarding the *ipilimumab treatment*, we need to examine a different jacobian matrix due to the presence of the extra term '$C\ X_2\ k_{lp}\ I_P^*$' in the second equation of the model. Therefore we obtain

$$J(E^{oo}) = \begin{pmatrix} r_2\ - C^o\ \frac{e_{CX}}{g_{CX}} - k_{lp}\ I_P^*\ C^o & 0 & 0 \\ \dots & \frac{e_{IC}\ i_0}{g_{IC}+i_0} - \mu_C - k_R\ R & -k_R C^o \\ \dots & 0 & -\mu_R \end{pmatrix}$$

with $p(\lambda) = -\left(r_2\ - C^o\ \frac{e_{CX}}{g_{CX}} - k_{lp}\ I_P^*\ C^o - \lambda\right)\left(\frac{e_{IC}\ i_0}{g_{IC}+i_0} - \mu_C - k_R\ R^o - \lambda\right)(\mu_R + \lambda)$.
Thus, its roots are

$$\begin{aligned} \lambda_1 &= r_2\ - C^o\ \frac{e_{CX}}{g_{CX}} - k_{lp}\ I_P^*\ C^o; \\ \lambda_2 &= \frac{e_{IC}\ i_0}{g_{IC}+i_0} - \mu_C - k_R\ R^o; \\ \lambda_3 &= -\mu_R; \end{aligned}$$

and the limiting system threshold value becomes $r_{BP}^{oo} = C^o\ \frac{e_{CX}}{g_{CX}} + k_{lp}\ I_P^*\ C^o$.

Positive equilibria

From the bifurcation point r_{BP}, a branch of positive equilibria appears and exists till r_{LP} is reached. Therefore when $r_2 \in [r_{LP}, r_{BP}]$ there exists an equilibria for which cancer is not eradicated. In order to better analyse the dynamic of the model, MatCont has been used.

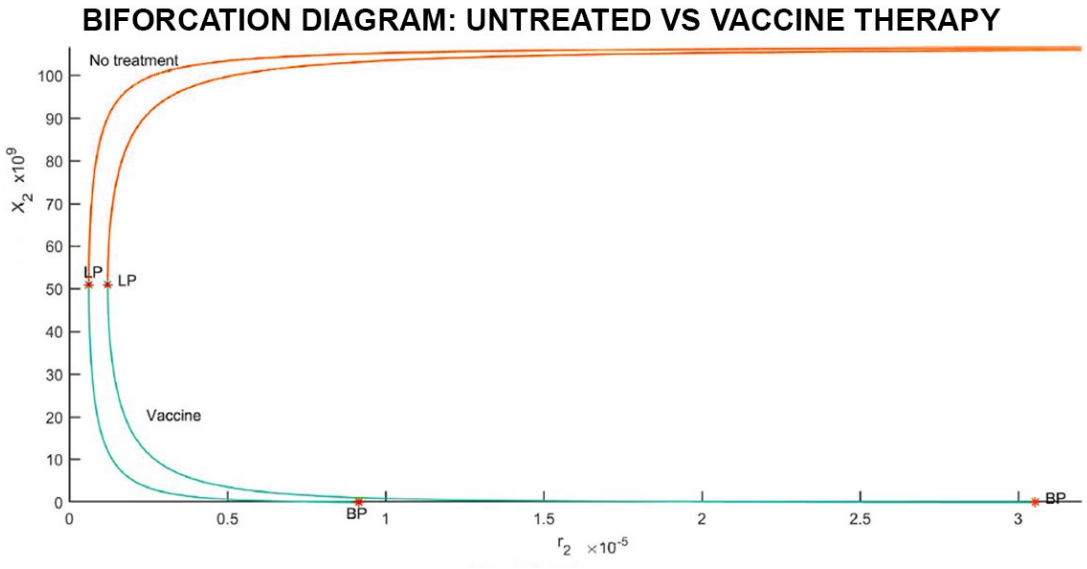

Figure 30: Bifurcation diagram no treatment vs vaccine therapy

Examining the bifurcation plots it is clear that other two equilibria are present inside the aforementioned interval: a high-tumor equilibrium, which is stable, and an unstable low-tumor one. Depending on the treatment the patient has been subjected to, the equilibrium points take different values. Specifically, figure 30 compares the no-therapy vs vaccine treatment: it is evident that dendritic cells administration does not relevantly change the dynamic of the system. Indeed, the critical points are only slightly moved to the right, but they still are not comparable with the order of magnitude of the real-data estimated r_2. Therefore, the high-tumor equilibrium is attractive for the majority of the initial conditions and this is not promising in terms of being able of eradicating the patient's cancer cells (more details could be found in Coletti's paper section 5.2).

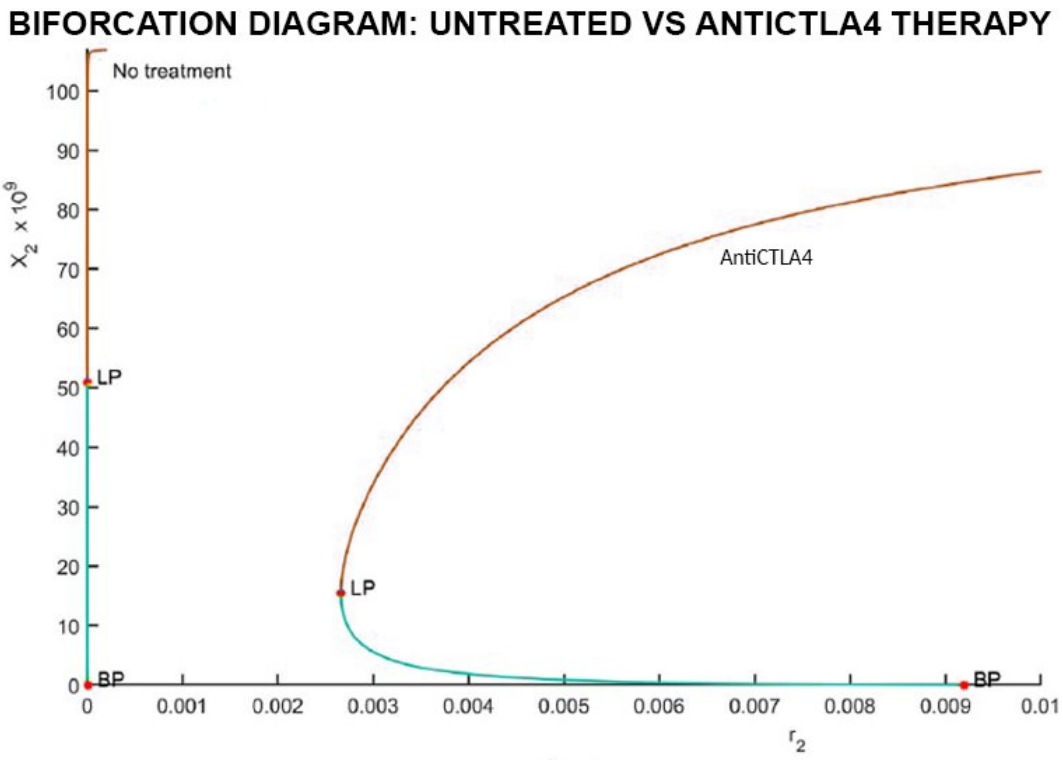

Figure 31: Bifurcation diagram no treatment vs AntiCTLA4 therapy

On the other hand, figure 31 displays the potential of ipilimumab drug. Under AntiCTLA4 therapy, r_2 limiting point and bifurcation point increase remarkably to an order comparable to the estimated value of X_2 proliferation rate parameter. Thus, this plot suggests tumor eradication could actually be possible; studying the basil of attraction of the equilibria will confirm this theory.

Furthermore, the numerical simulations run above show that the quantity and the administration schedule highly influence the therapy results changing the dynamic of the system (see figure 32). In particular, what seams to be the best scenario is the androgen deprivation therapy coupled with ipilimumab drug. These combined treatments, supplied together, could bring the system to the no-tumor steady state thus resulting into the removal of all the cancer cells and the complete eradication of the cancer. Further analysis can be found on Coletti's paper but additional research has to be run in order to extend the model and validate it on more realistic data.

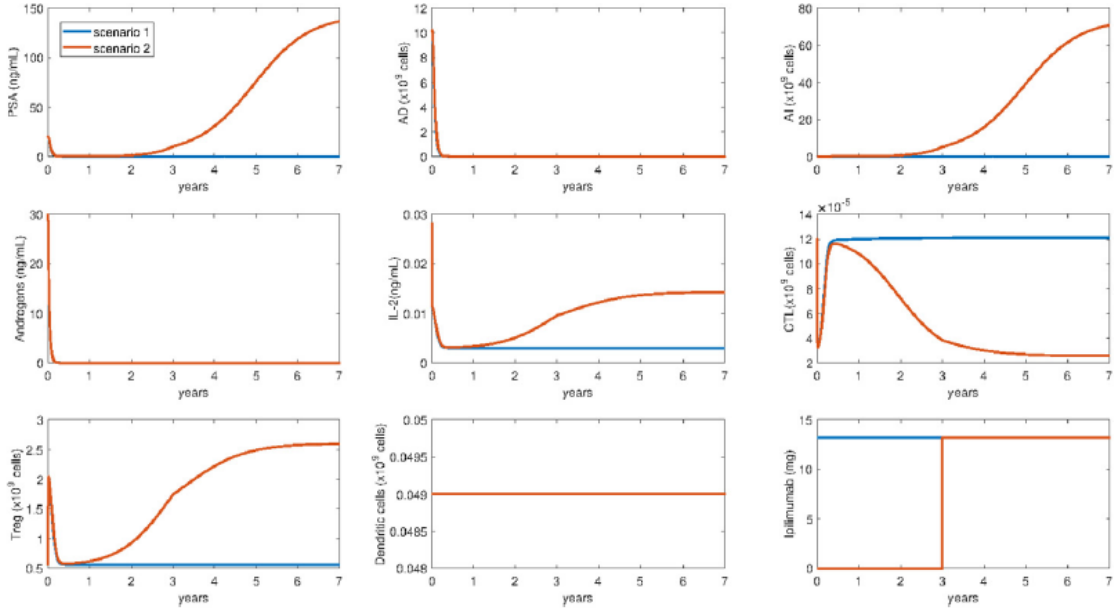

Figure 32: Androgen deprivation and AntiCTLA4 therapy combined (scenario 1) vs separated administration time (scenario 2)

3 Results and conclusions

Considered variables

1) **First Model**

- $T(t)$: tumor cell population.
- $N(t)$: total NK cell population. Natural killer cells, also known as NK cells or large granular lymphocytes (LGL), are a type of cytotoxic lymphocyte critical to the innate immune system that belong to the rapidly expanding family of known innate lymphoid cells (ILC) and represent 5–20 percent of all circulating lymphocytes in humans. The role of NK cells is analogous to that of cytotoxic T cells in the vertebrate adaptive immune response. NK cells provide rapid responses to virus-infected cell and other intracellular pathogens acting at around 3 days after infection, and respond to tumor formation.
- $L(t)$: total $CD8^+$T cell population. A cytotoxic T cell (also known as TC, cytotoxic T lymphocyte, CTL, T-killer cell, cytolytic T cell, $CD8^+$T-cell or killer T cell) is a T lymphocyte (a type of white blood cell) that kills cancer cells, cells that are infected by intracellular pathogens (such as viruses or bacteria), or cells that are damaged in other ways.
- $C(t)$: number of circulating lymphocytes. A lymphocyte is a type of white blood cell (leukocyte) in the immune system of most vertebrates. Lymphocytes include natural killer cells (which function in cell-mediated, cytotoxic innate immunity), T cells (for cell-mediated, cytotoxic adaptive immunity), and B cells (for humoral, antibody-driven adaptive immunity). They are the main type of cell found in lymph, which prompted the name "lymphocyte". Lymphocytes make up between 18% and 42% of circulating white blood cells.
- $M(t)$: chemotherapy drug concentration in the bloodstream.
- $I(t)$: immunotherapy drug concentration in the bloodstream.

2) **Second Model**

- $X_1(t)$: Androgen Dependent Prostate Cancer cells (ADPC). Prostate cancer that needs androgens (male hormones) to grow and therefore stops growing when androgens are not present. Many early-stage prostate cancers are androgen-dependent, so reducing the amount of androgens in the body or blocking their action may be an effective type of therapy. Also called androgen-sensitive prostate cancer, castrate-sensitive prostate cancer, CSPC, hormone-sensitive prostate cancer, and HSPC.
- $X_2(t)$: Androgen Independent Prostate Cancer cells (AIPC). Each year, an estimated 25,000 men will find out their prostate cancer has changed enough to become resistant to standard androgen-deprivation therapy, also called hormone therapy. At this point, the cancer is classified as androgen-independent prostate cancer (AIPC) or hormone-refractory prostate cancer, meaning that the cancer is still able to thrive despite hormone treatment.
- $C(t)$: circulating Cytotoxic T Lymphocytes (CTL).
- $R(t)$: circulating Treg cells (Treg). Regulatory T cells (Tregs) are a specialized subpopulation of T cells that act to suppress immune response, thereby maintaining homeostasis and self-tolerance. It has been shown that Tregs are able to inhibit T cell proliferation and cytokine production and play a critical role in preventing autoimmunity. Different subsets with various functions of Treg cells exist. Tregs can be usually identified by flow cytometry. The most specific marker for these cells is FoxP3, which is localized intracellulary. Selected surface markers such as CD25high (high molecular density) and CD127low (low molecular density) could serve as surrogate markers to detect Tregs in a routine clinical practice. Dysregulation in Treg cell frequency or functions may lead to the development of autoimmune disease. Therapeutical Treg modulation is considered to be a promising therapeutical approach to treat some selected disorders, such as allergies, and to prevent allograft rejection.
- $I_L(t)$: interleukin-2 in blood. Interleukin-2 (IL-2) is an interleukin, a type of cytokine signaling molecule in the immune system. It is a 15.5–16 kDa protein that regulates the activities of white blood cells (leukocytes, often lymphocytes) that are responsible for immunity. IL-2 is part of the body's natural response to microbial infection, and in discriminating between foreign ("non-self") and "self". IL-2 mediates its effects by binding to IL-2 receptors, which are expressed by lymphocytes. The major sources of IL-2 are activated $CD4^+$T cells and activated $CD8^+$T cells.
- $D(t)$: circulating Dendritic cells. Dendritic cells (DCs) are antigen-presenting cells (also known as accessory cells) of the mammalian immune system. Their main function is to process antigen material and present it on the cell surface to the T cells of the immune system. They act as messengers between the innate and the adaptive immune systems.
- $A(t)$: Androgen concentration.

– $I_P(t)$: Ipilimumab drug.

1) **First Model**

– T for tumor cells

– N, L, C in immune system

– M, I for treetments

2) **Second Model**

– X_1, X_2 are cancer cells

– C, R, I_L, D are in immune system

– A, I_P are as treetments

Remark. In both models, the growth of tumors (T, X_1, X_2) is assumed to be logistic.

Equilibria and stability

In both models, the important equilibrium (if exists) is the tumor-free equilibrium. As mentioned in papers, tumor-free equilibrium exists but it is not stable and there are some bifurcations.

1) **First Model**
The tumor-free equilibrium is $E_0 = (T_{E,1}, N_E, L_E, C_E) = (0, 1/\beta f, 0, 1/\beta)$. E_0 is stable if and only if $c > \beta f$, where c represents the NK cells kill rate.
According to the paper, we have another bifurcation related to j parametere which by increasing j, E_0 is converted from unstable to semi stable.

2) **Second Model**
If we set $X_2^0 = 0$ then the tumor-free equilibrium is $E_0 = (X_2^0 = 0, C^0, R^0)$ if $\mu_C K_R R^0 > \dfrac{e_{IC} i_0}{g_{IC} + i_0}$. E_0 is stable if and only if $r_2 < C_0 \dfrac{e_{CX}}{g_{CX}}$.
Regarding the ipilimumab treatment, E_0 is stable if and only if $r_2 < C_0 \dfrac{e_{CX}}{g_{CX}} + k_{lp} I_P^* C^0$.

Treatments

1) **First Model**

– **Immune system response**. The healthy innate immune response is sufficiently strong to control the tumor. However, when the immune system is weakened, a tumor of the same size grows to a dangerous level in the absence of treatment interventions.

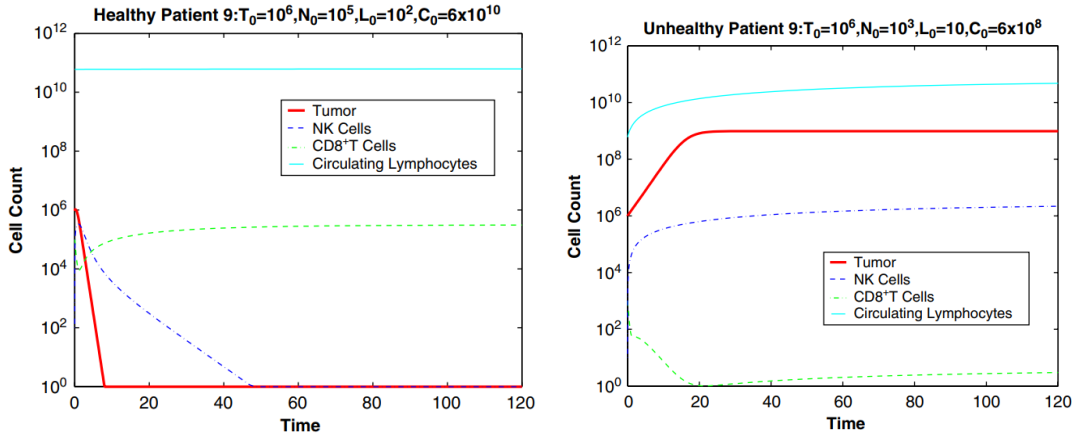

Figure 33: Comparison between healthy and unhealthy patient.

– **Chemotherapy**. This treatment can be administrated only after the tumor is large enough to be considered potentially detectable. Also it is sensitive to the chemotherapy dosing regimen.

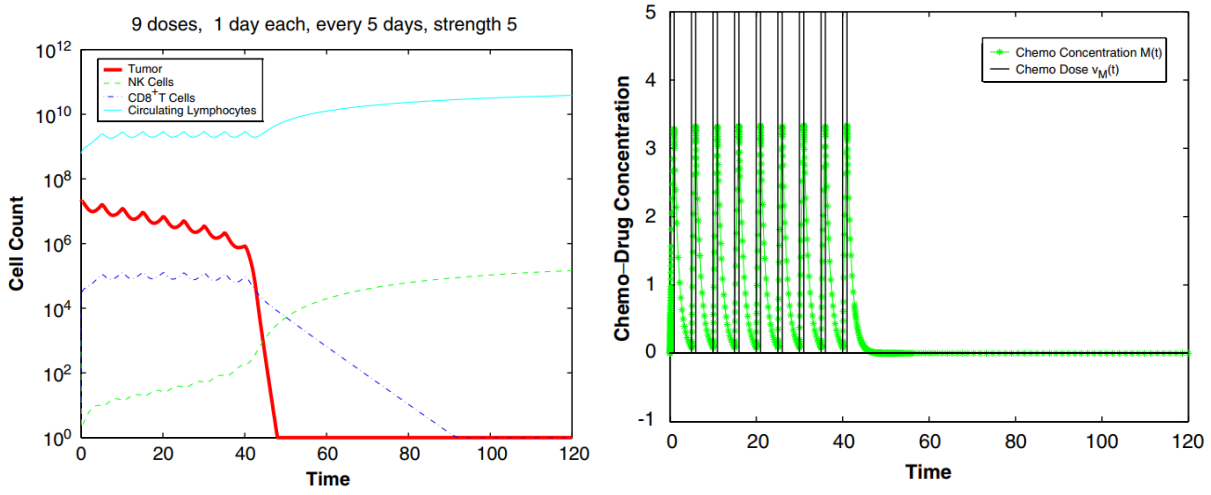

Figure 34: Chemotherapy is sufficient.

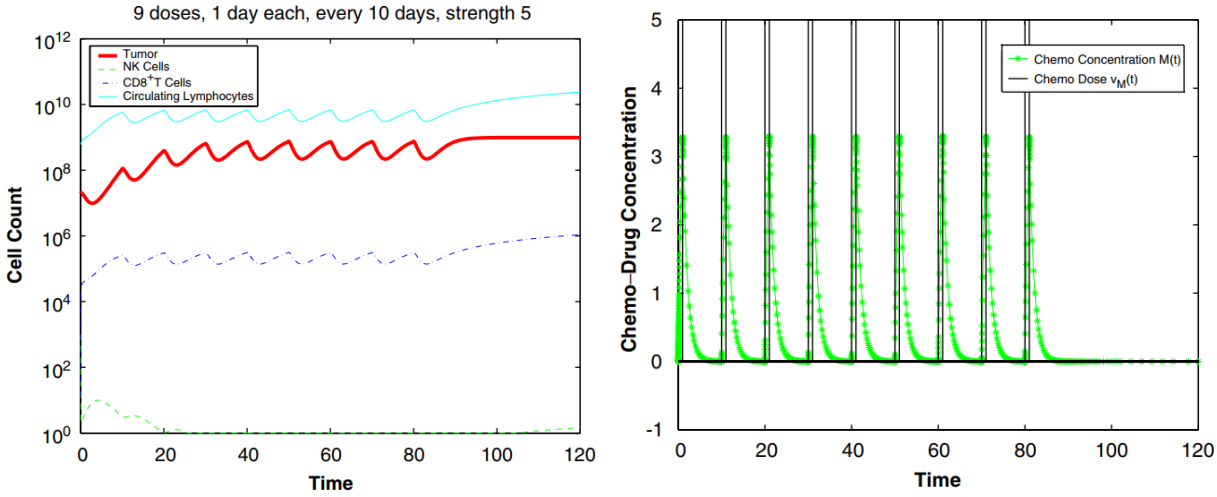

Figure 35: Chemotherapy is not sufficient.

– **Immunotherapy**. The advantage of this treatment is that the immune system is directly strengthened, and not depleted as it is with chemotherapy. But the effectiveness may be limited to smaller tumor sizes.

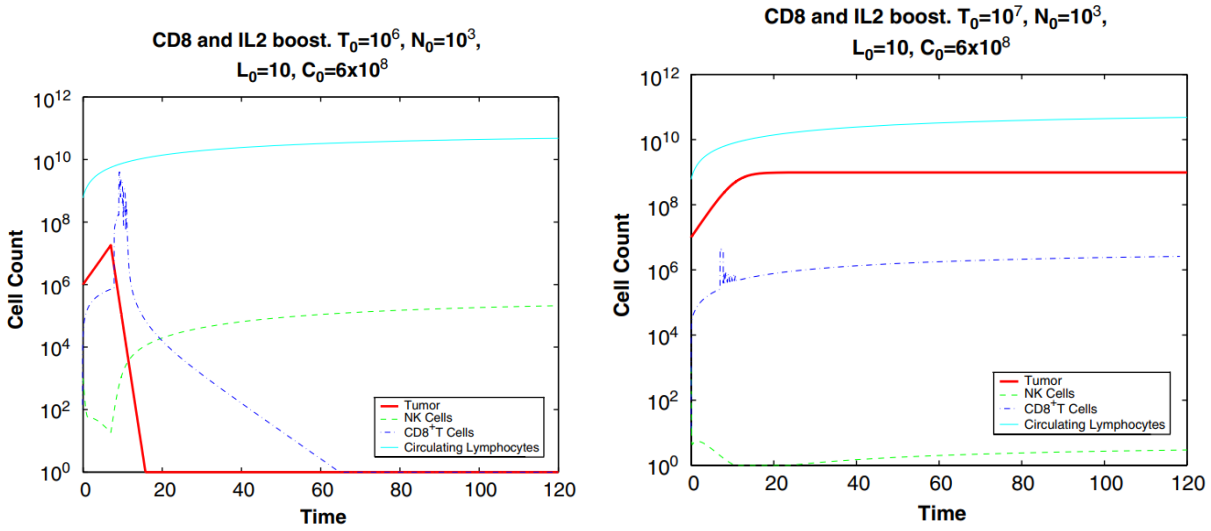

Figure 36: Left: Immunotherapy is sufficient. Right: Immunotherapy is not sufficient.

– **Combination therapy**. This treatment consists of an administration of chemotherapy and immunother-

apy. This allows less chemotherapy (which causes damage to the body) to be administered while keeping immune cell counts high. This therapy fails for large tumors unless different dosages and periods of administration of both chemotherapy and immunotherapy are adopted.

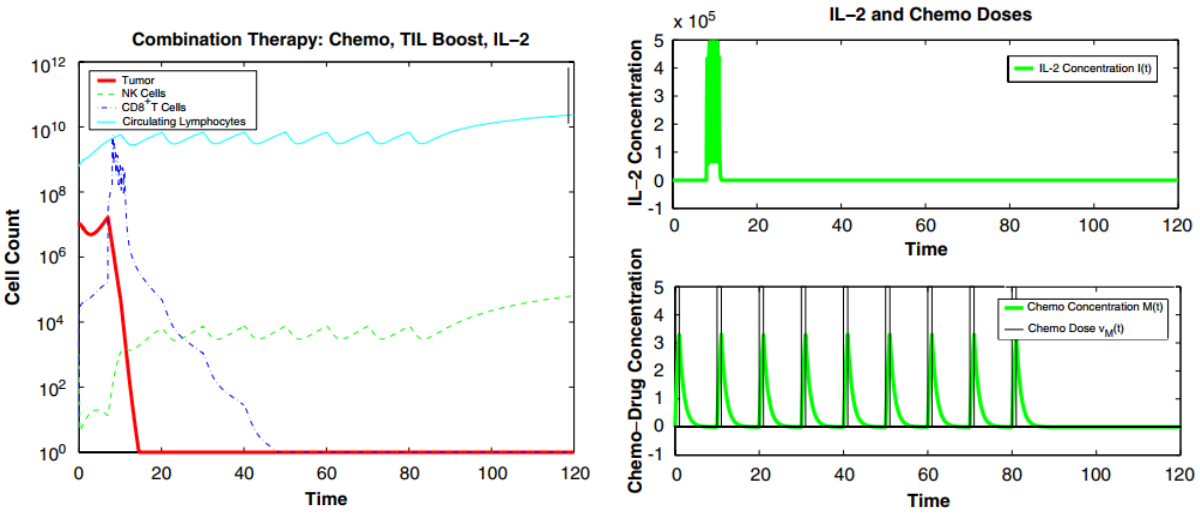

Figure 37: Combination therapy is sufficient. $T_0 = 2 \times 10^7$; $N_0 = 10^3$; $L_0 = 10$; $C_0 = 6 \times 10^8$; $I_0 = 0$; $M_0 = 0$. Two immunotherapy doses are administered at the beginning for a duration of 4 time unit, $v_I = 5 \times 10^5$. Five chemotherapy doses are administered for a duration of 7 time unit, $v_M = 3$.

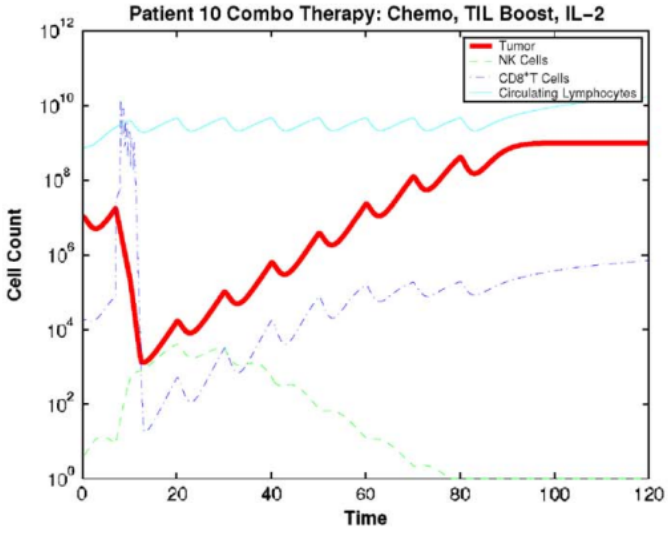

Figure 38: Combination therapy is not sufficient. $T_0 = 10^7$; $N_0 = 10^3$; $L_0 = 10$; $C_0 = 6 \times 10^8$; $I_0 = 0$; $M_0 = 0$. Two immunotherapy doses are administered in 2 time unit, $v_I = 10^9$, then six immunotherapy doses are administered during 4 time unit, $v_I = 5 \times 10^6$. Nine chemotherapy doses are administered once every 10 days for a duration of 1 time unit, $v_M = 5$.

– **Vaccine therapy** This is a special case of immunotherapy for treating cancer. Combination of chemotherapy and vaccine can kill a tumor, but it depends on the size of tumor, doses of chemotrapy and the time of starting the vaccination. There are cases for which vaccine therapy alone is able to control a growing tumor and again, it sensetive to the size of tumor and the time of starting the vaccination.

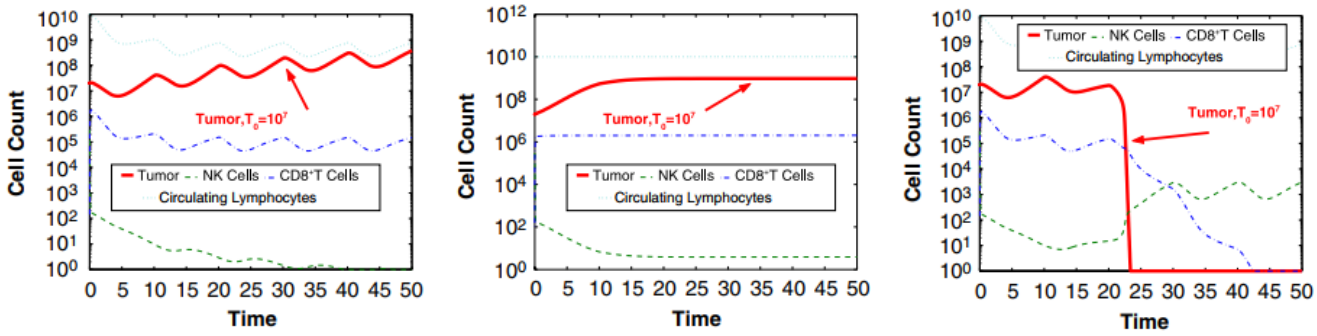

Figure 39: $T_0 = 2 \times 10^7$; $N_0 = 3 \times 10^5$; $L_0 = 100$; $C_0 = 10^{10}$. Left: $v_M = 2$ administered for 3 consecutive days every 10 days. Center: vaccine is administered at day 10, $c = 7.131 \times 10^{-9}$; $g = 0.5$; $j = 1$; $s = 0,0019$; $d = 15$. Right: combination of the two previous therapies.

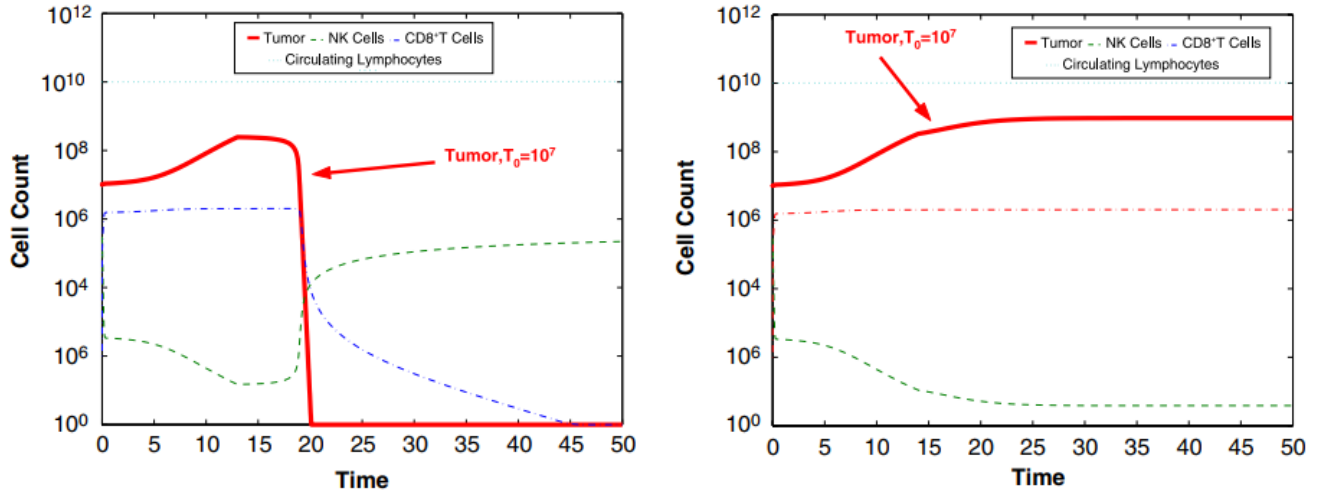

Figure 40: $T_0 = 10^7$; $N_0 = 3 \times 10^5$; $L_0 = 100$; $C_0 = 10^{10}$. Left: vaccine is administered at day 13. Right: vaccine is administered at day 14. In both cases the vaccine is modeled as: $c = 7.131 \times 10^{-9}$; $g = 0.5$; $j = 1$; $s = 0,0019$; $d = 15$.

2) **Second Model**

- **Immune system response**. In this case, ADPC cancer cells increase, until reaching a constant threshold value. Simultaneously, PSA reaches its maximum level while there is no AIPC creation since there is no pressure into the androgen-independent cancer form.

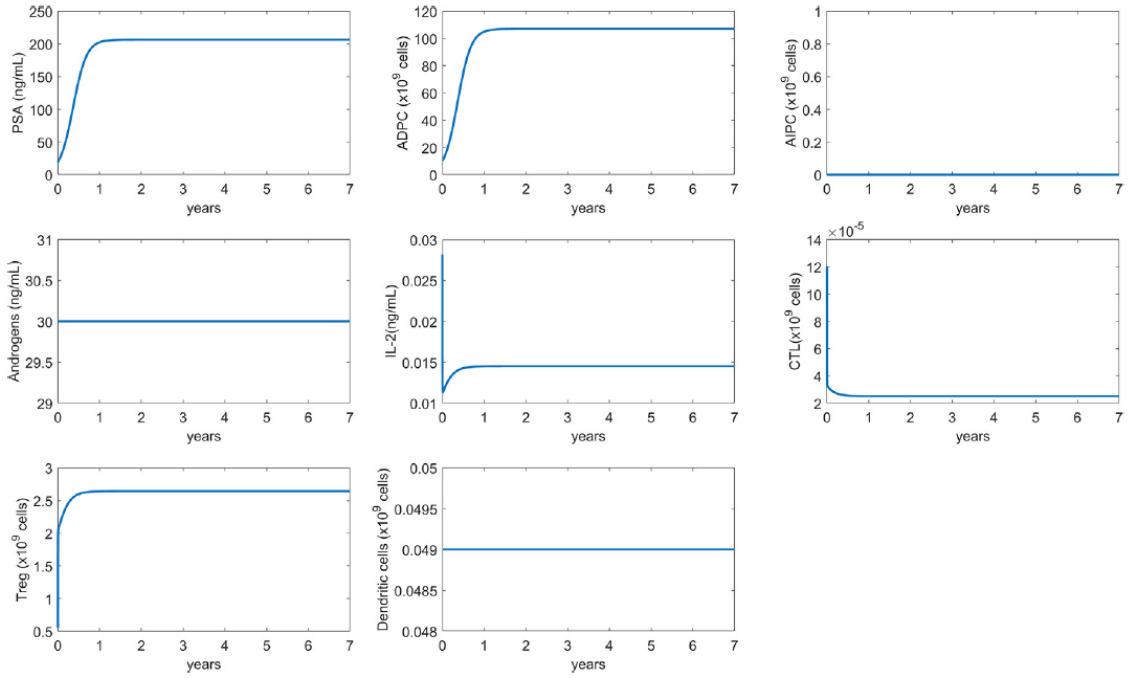

Figure 41: No drugs nor other therapies have been taken to deal with the tumor. $v = 0$, $I_{CX} = 0$ and $I_P(0) = 0$.

- **Androgen deprivation**. In this case, PSA level first decreases due to the destruction of ADPC, but it secondly starts increasing again due to the selection of androgen independent cancer form.
- **Combination of androgen deprivation and dendritic cells vaccine**. Dendritic cells injection helps the immune system to increase CTL and Treg values, but the variables PSA, ADPC and AIPC do not show any relevant differences compared to the last case and the result is still the spread of the cancer.

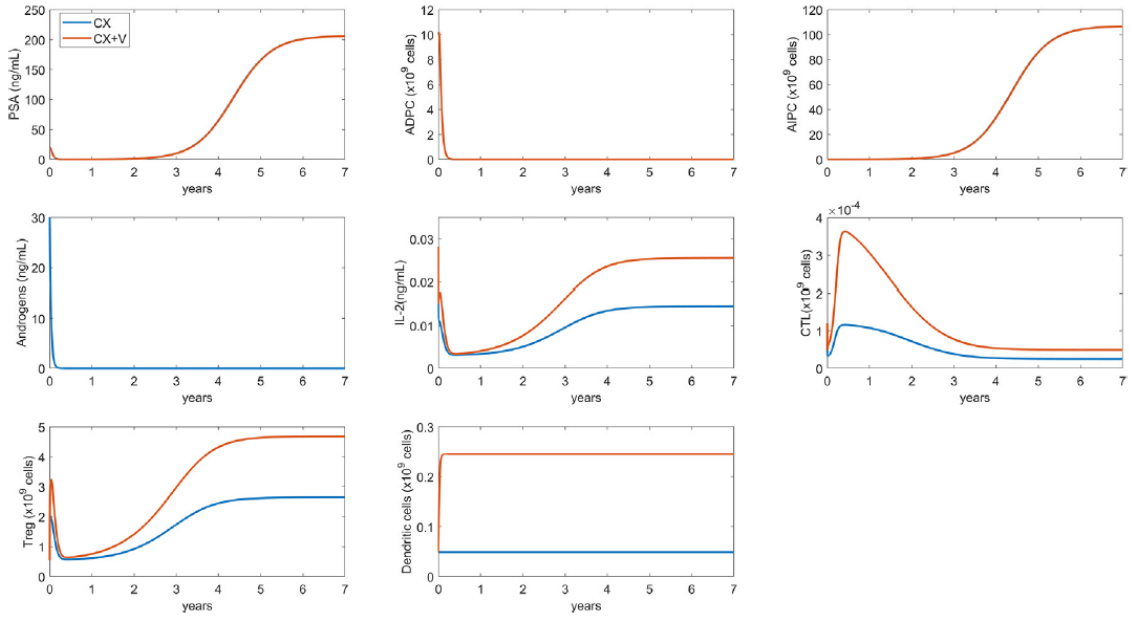

Figure 42: Androgen deprivation therapy by itself (blue) and combined with the vaccine treatment (orange)

- **Combination of androgen deprivation and Anti-CTLA4 (ipilimumab injection)**. Results are different depending on the schedules and the doses of the drug. But, no matter of the AntiCTLA4 drug dose, PSA level will start to increase again and the high-tumor level will be reached soon or later.
  Choosing a repeated intermittent treatment with a low dose returns better simulations results. Anyway, this still is not enough to eradicate the cancer. An early administered treatment with repeated and intermittent ipilimumab injections in combination with androgen deprivation therapy causes a better tumor control where, as the therapy starts, ADPC suddenly disappear and AIPC's value oscillates tending to the no-tumor point.

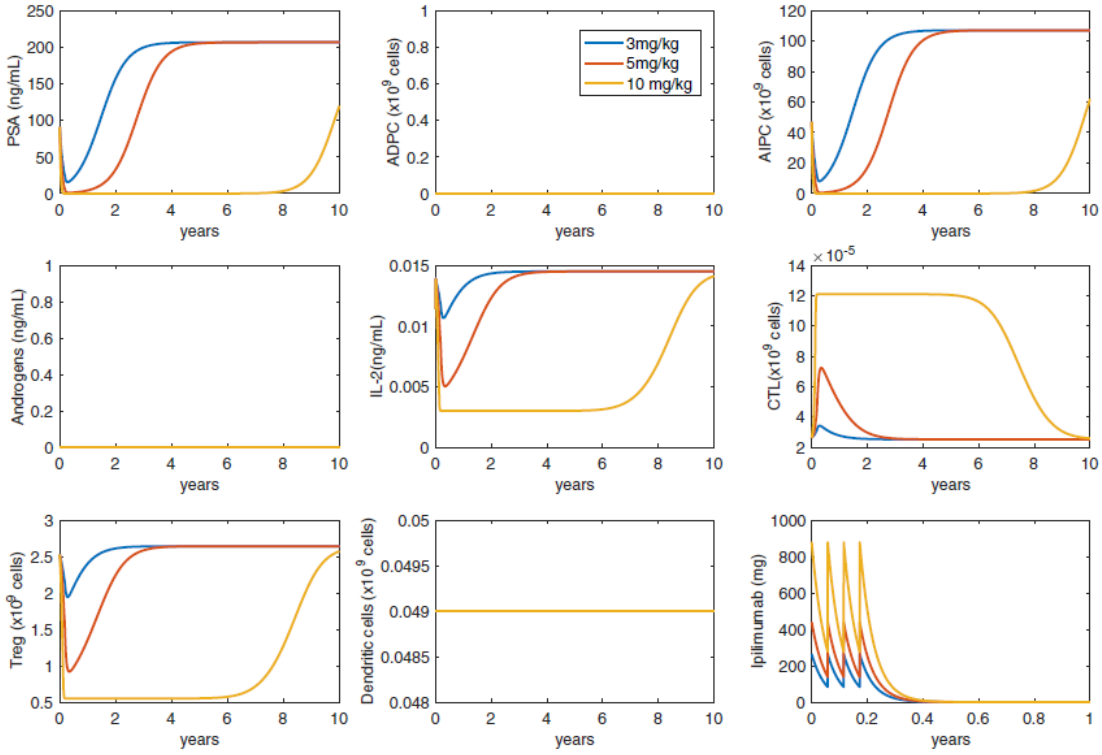

Figure 43: Androgen deprivation therapy combined with intermittent ipilimumab injection in different doses

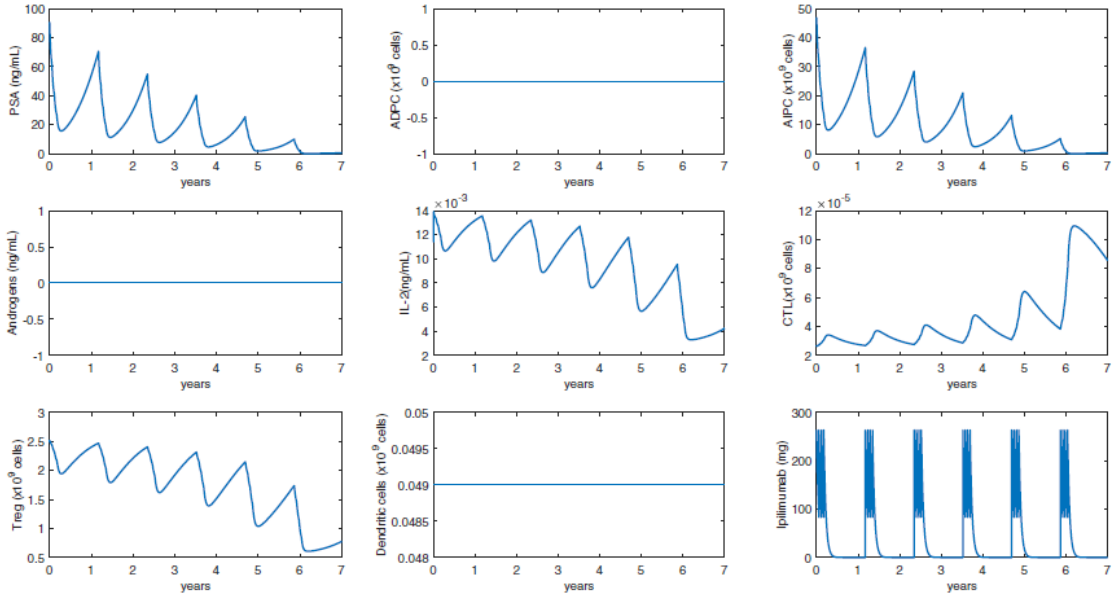

Figure 44: Androgen deprivation therapy combined with repeated intermittent ipilimumab injections

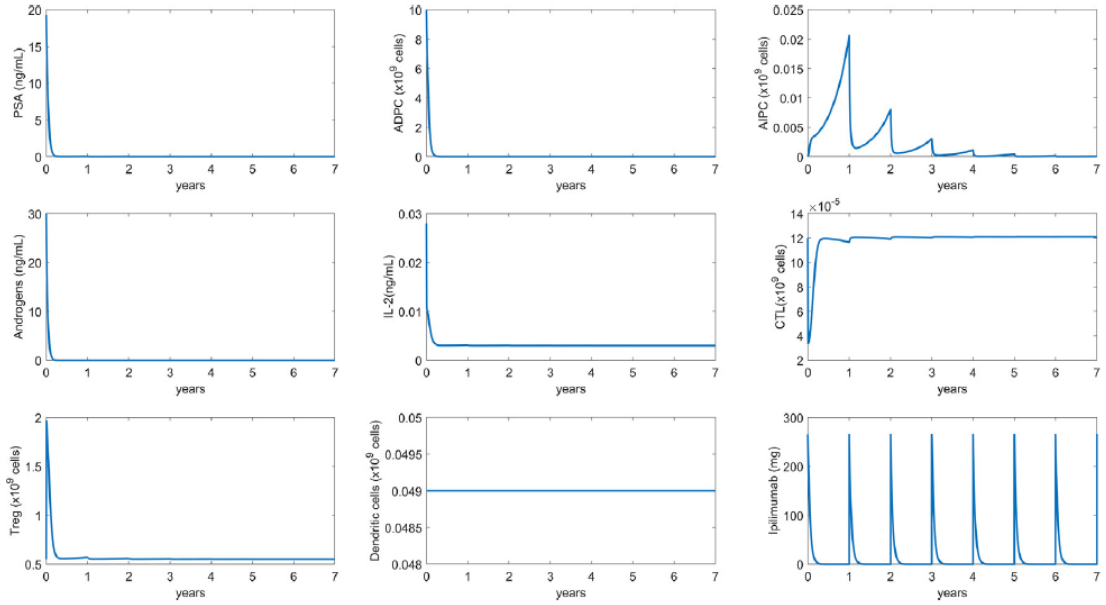

Figure 45: Androgen deprivation therapy combined with early administered and repeated intermittent ipilimumab injections